https://doi.org/10.5194/bg-2019-266
Preprint. Discussion started: 8 August 2019

Biogeosciences
Discussions
Open Access
EGU

Seawater pH reconstruction using boron isotopes in multiple planktonic foraminifera species with different depth habitats and their potential to constrain pH and pCO_2 gradients

Maxence Guillermic[1,6], Sambuddha Misra[2,3], Robert Eagle[1,5], Alexandra Villa[6], Fengming Chang[4], Aradhna Tripati [1,5,6]

[1] Laboratoire Géosciences Océan UMR6538, UBO, Institut Universitaire Européen de la Mer, Rue Dumont d'Urville, 29280, Plouzané, France
[2] The Godwin Laboratory for Palaeoclimate Research, Department of Earth Sciences, University of Cambridge, UK
[3] Indian Institute of Science, Centre for Earth Sciences, Bengaluru, Karnataka 560012, India
[4] Key Laboratory of Marine Geology and Environment, Institute of Oceanology, Chinese Academy of Sciences, Qingdao 266071, China
[5] Institute of the Environment and Sustainability, Department of Atmospheric and Oceanic Sciences, University of California – Los Angeles, CA 90095, USA
[6] Department of Earth, Planetary, and Space Sciences, UCLA, University of California – Los Angeles, Los Angeles, CA 90095 USA

Submitted to Biogeosciences

*Corresponding author:
E-mail address: maxence.guillermic@gmail.com

https://doi.org/10.5194/bg-2019-266
Preprint. Discussion started: 8 August 2019

Biogeosciences Discussions
Open Access
EGU

ABSTRACT

Boron isotope systematics of planktonic foraminifera from core-top sediments and culture experiments have been studied to investigate the sensitivity of $\delta^{11}B$ of their calcite tests to seawater pH. However, our knowledge of the relationship between $\delta^{11}B$ and pH remains incomplete for several taxa. Thus, to expand the potential scope of application of this proxy, we report data for 7 different species of planktonic foraminifera from sediment core-tops. We utilize a method for the measurement of small samples of foraminifera and calculate the $\delta^{11}B$-calcite sensitivity to pH for *Globigerinoides ruber*, *Trilobus sacculifer* (sacc or w/o sacc), *Orbulina universa*, *Pulleniatina obliquiloculata*, *Neogloboquadrina dutertrei*, *Globorotalia menardii* and *Globorotalia tumida*, including for unstudied coretops and species. The sensitivity of $\delta^{11}B_{carbonate}$ to $\delta^{11}B_{borate}$ (eg. $\Delta\delta^{11}B_{carbonate}/\Delta\delta^{11}B_{borate}$) in core-tops is close to unity. Deep-dwelling species closely follow the core-top calibration for *O. universa*, which is attributed to respiration-driven microenvironments, likely caused by light limitation for symbiont-bearing foraminifera. These taxa have diverse ecological preferences and are from sites that span a range of oceanographic regimes, including some that are in regions of air-sea equilibrium and others that are out of equilibrium with the atmosphere. Our data support the premise that utilizing boron isotope measurements of multiple species within a sediment core can be utilized to constrain vertical profiles of pH and pCO_2 at sites spanning different oceanic regimes, thereby constraining changes in vertical pH gradients and yielding insights into the past behavior of the oceanic carbon pump.

https://doi.org/10.5194/bg-2019-266
Preprint. Discussion started: 8 August 2019

63 **1. Introduction**

64 The oceans are absorbing a substantial fraction of anthropogenic carbon emissions resulting in a steady
65 decline in seawater pH (Fig. 1; IPCC, 2014). Yet there is a considerable uncertainty over the magnitude of future
66 pH change in different parts of the ocean and the response of marine biogeochemical cycles to physio-chemical
67 parameters (T, pH) caused by climate change (Bijma et al., 2002; Ries et al., 2009). Therefore there is an
68 increased interest in reconstructing past seawater pH (Hönisch and Hemming, 2005; Liu et al., 2009; Wei et al.,
69 2009; Douville et al., 2010), in understanding spatial variability in aqueous pH and carbon dioxide (pCO_2)
70 (Foster et al., 2008; Martinez-Boti et al., 2015; Raitzsch et al., 2018), and in studying the response of the
71 biological carbon pump utilizing geochemical proxies (Yu et al., 2007, 2010, 2016).

72 Although proxies for carbon cycle reconstruction are complex in nature (Pagani et al., 2005; Tripati et
73 al., 2009, 2011; Allen and Hoenisch, 2012), the boron isotope composition of foraminiferal tests is emerging as
74 one of the more robust candidates (Hönisch et al., 2005, 2009; Ni et al., 2007; Foster et al., 2008, 2012; Bartoli et
75 al., 2011; Henehan et al., 2013; Martinez-Boti et al., 2015; Chalk et al., 2017). The study of laboratory cultured
76 foraminifera has demonstrated a systematic dependence of the boron isotope composition of tests on ambient pH
77 (Sanyal et al., 1996, 2001; Henehan et al., 2013, 2016). Core-top measurements on globally distributed samples
78 also show a $\delta^{11}B$ sensitivity to pH with taxon-specific offsets from the theoretical fractionation line of borate ion
79 (Rae et al., 2011; Henehan et al., 2016; Raitzsch et al., 2018).

80 Knowledge of seawater pH, in conjunction with constraints on one other carbonate system parameter
81 (Total Alkalinity (TA), DIC, $[HCO_3^-]$, $[CO_3^{2-}]$), can be utilized to constrain aqueous pCO_2. Application of
82 empirical calibrations for boron isotopes, determined for select species of foraminifera from core-tops and
83 laboratory cultures, has resulted in accurate reconstructions of pCO_2 utilizing downcore samples from sites that
84 are in quasi-equilibrium with the atmosphere at present. $\delta^{11}B_{carbonate}$ based reconstructed values of pCO_2 are
85 analytically indistinguishable from ice core CO_2 records (Hönisch et al., 2005, 2009; Foster et al., 2008;
86 Henehan et al., 2013; Chalk et al., 2017).

87 Therefore the last decade has produced several studies aiming at reconstructing past seawater pH using
88 boron isotopes to constrain atmospheric pCO_2 in order understand the changes in the global carbon cycle
89 (Hönisch et al., 2005, 2009; Foster et al., 2008, 2012, 2014; Seki et al., 2010; Bartoli et al., 2011; Rae et al.,
90 2011; Henehan et al., 2013; Martinez-Boti et al., 2015; Chalk et al., 2017). In addition to reconstructing
91 atmospheric pCO_2, in a few studies, the $\delta^{11}B$ proxy has been applied to mixed-layer planktonic foraminifera at
92 sites out of equilibrium with the atmosphere to constrain past air-sea fluxes (Foster et al., 2014; Martinez-Boti et
93 al., 2015). A small body of work has examined whether data for multiple species in core-top (Foster et al., 2008)
94 and down-core samples could be used to constrain vertical profiles of pH through time (Palmer et al., 1998;
95 Pearson and Palmer, 1999).

96 This study aims to improve the growing pool of information using empirical data for planktonic
97 foraminifera to constrain boron isotope systematics. We make critical additions to the emerging pool of data of
98 core-top planktonic foraminifera from different oceanographic regimes, including data for species that have not
99 previously been examined. We utilize a low-blank (15 pg B to 65 pg B), high precision (2sd on the international
100 standard JCP-1 is 0.20 ‰, n=6) $\delta^{11}B_{carbonate}$ analysis method (down to ~250 µg CaCO3), modified after Misra et
101 al. (2014), to study multiple species of planktonic foraminifera from sediment coretops that span a range of
102 oceanographic regimes, including open-ocean oligotrophic settings and marginal seas. We constrain calibrations

https://doi.org/10.5194/bg-2019-266
Preprint. Discussion started: 8 August 2019

for different species, and compare results to published work (Foster et al., 2008; Henehan et al., 2013; Henehan et al., 2016; Martinez-Boti et al., 2015; Raitzsch et al., 2018). We also test whether these data support the application of boron isotope measurements of multiple species within a sediment core as a proxy for constraining vertical profiles of pH and pCO_2.

2. Background

2.1 Planktonic foraminifera as archives of seawater pH

Planktonic foraminifera are used as archives of past environmental conditions within the mixed layer and thermocline, as their chemical composition is correlated with the physio-chemical parameters of their calcification environment (Ravelo and Fairbanks, 1992; Elderfield and Ganssen, 2000; Dekens et al., 2002; Anand et al., 2003; Sanyal et al., 2001; Ni et al., 2007; Henehan et al., 2013, 2015, 2016; Howes et al., 2017; Raitzch et al., 2018). The utilization of geochemical data for multiple planktonic foraminifera species with different ecological preferences to constrain vertical gradients has been explored in several studies. The framework for such an approach was first developed using modern samples of planktonic foraminifera for oxygen isotopes, where it was proposed as a tool to constrain vertical temperature gradients and study physical oceanographic conditions during periods of calcification (Ravelo and Fairbanks, 1992). Similarly, vertical temperature and water $\delta^{18}O$ profiles were reconstructed for the Paleocene-Eocene Thermal Maximum using Mg/Ca and carbonate $\delta^{18}O$ ratios in planktonic and benthic foraminifera (Tripati and Elderfield, 2005).

Planktonic foraminifera species complete their lifecycle in a particular depth habitat due to their ecological preference (Ravelo and Fairbanks, 1992; Farmer et al., 2007), it is thus theoretically possible to reconstruct water column profiles of pH using data from multiple taxa (Palmer and Pearson, 1998; Anagnostou et al., 2016). The potential use of an analogous approach to reconstruct past profiles of seawater pH was perhaps first highlighted by Palmer and Pearson (1998) on Eocene samples to constrain pH-depth gradients. However, in these boron isotope-based studies, it was assumed that boron isotope offset from seawater and foraminiferal carbonate were constant, which is an assumption not supported by subsequent studies (e.g., Hönisch et al., 2003; Foster et al., 2008; Henehan et al., 2013, 2016; Raitszch et al., 2018; Rae, 2018). The existence of species-level differences makes the acquisition of more modern, coretop and culture data and testing of this framework for boron isotopes essential for effective application of the proxy.

2.2 Boron systematics in seawater

Boron is a conservative element in seawater with a long residence time (τ_B ~ 14 Myr) (Lemarchand et al., 2002a). In seawater, boron exists as trigonal boric acid $B(OH)_3$ and tetrahedral borate ion $B(OH)_4^-$ (borate). The relative abundance of boric acid and borate ion is a function of the ambient seawater pH. At standard open ocean conditions (T = 25 °C and S = 35), the dissociation constant of boric acid is equal to 8.60 (Dickson, 1990), implying that boron mainly exists in the form of boric acid in seawater. Since the pK_B and seawater pH (e.g., ~8.1, NBS) values are similar, it implies that small changes in seawater pH will induce strong variations in the abundance of the two boron species (Fig. 2).

Boron has two stable isotopes, ^{10}B and ^{11}B, with average relative abundances of 19.9 and 80.1 %, respectively. Variations in B isotope ratio are expressed in conventional delta (δ) notation:

https://doi.org/10.5194/bg-2019-266
Preprint. Discussion started: 8 August 2019

$$\delta^{11}B\ (‰) = 1000 \times \left(\frac{^{11}B/^{10}B_{Sample}}{^{11}B/^{10}B_{NIST\ 951\text{-}a}} - 1 \right) \quad (1)$$

where positive values represent enrichment in the heavy isotope ^{11}B, and negative values enrichment in the light isotope ^{10}B, relative to the standard reference material. Boron isotope values are reported versus the NIST SRM 951 (Cantazaro et al., 1970).

$B(OH)_3$ is enriched in ^{11}B compared to $B(OH)_4^-$ with a constant offset between the two chemical species, within the range of physio-chemical variation observed in seawater, given by the fraction factor (α). This fractionation factor (α) between $B(OH)_3$ and $B(OH)_4^-$ of 27.2 ± 0.6 ‰ has been empirically determined by Klochko et al., (2006) in seawater. Note, Nir et al., (2015) calculate this fractionation factor, using an independent method, to be 26 ± 1 ‰, which is within the analytical uncertainty of the Klochko et al., (2006) value.

2.3 Boron isotopes in planktonic foraminifera calcite

Many biogenic carbonate-based geochemical proxies are affected by "vital effects" or biological fractionations (Urey et al., 1951). The $\delta^{11}B_{carbonate}$ in foraminifera exhibits species-specific offsets (see Rae et al., 2018 for review) compared to theoretical predictions for the boron isotopic composition of $B(OH)_4^-$ (α=1.0272, Klochko et al., 2006). As the analytical and technical aspects of boron isotope measurements have improved (Foster et al., 2008; Rae et al., 2011; Misra et al., 2014; Lloyd et al., 2018), evidence for taxonomic differences have not been eliminated, but have become increasingly apparent (Foster et al., 2008, 2018; Henehan et al 2013, 2016; Noireaux et al., 2015; Foster et al., 2016; Rae et al., 2018; Raitzsch et al., 2018).

At present, culture and core-top calibrations have been published for several planktonic species including *Trilobatus sacculifer*, *Globigerinoides ruber*, *Globigerina bulloides*, *Neogloboquadrina pachyderma*, *Orbulina universa* (Foster et al., 2008; Henehan et al., 2013; Henehan et al., 2015; Sanyal et al., 1996; Sanyal et al., 2001; Yu et al., 2013, Raitzsch et al., 2018) as well as multiple benthic foraminiferal species (Hönisch et al., 2008, Rae et al., 2011; Yu et al., 2010). Although the boron isotopic composition of several species of foraminifera are now commonly used tools for reconstructing surface seawater pH, for other species, there is a lack of data constraining boron isotope offsets between foraminiferal carbonate and borate ion in seawater.

2.4 Origin of biological fractionations in foraminifera

Perforate foraminifera are calcifying organisms that maintain a large degree of biological control over their calcification space, and thus, mechanisms of biomineralization may be of significant importance in controlling the $\delta^{11}B$ of the biogenic calcite. The biomineralization of foraminifera is based on seawater vacuolization (Erez, 2003; de Nooijer et al., 2014) with parcels of seawater being isolated by an organic matrix thereby creating a vacuole filled with seawater. Recent work has also demonstrated that even if the chemical composition of the reservoirs is modified by the organism, seawater is directly involved in the calcification process with vacuoles formed at the periphery of the shell (de Nooijer et al., 2014). Culture experiments by Rollion-Bard and Erez., (2010) have proposed that the pH at the site of biomineralization is elevated to an upper pH limit of ~9 for the species *Amphistegina lobifera* which would support a pH modulation of a calcifying fluid in foraminifera.

https://doi.org/10.5194/bg-2019-266
Preprint. Discussion started: 8 August 2019

For taxon with symbionts, the microenvironment surrounding the foraminifera is chemically different from seawater due to photosynthetic activity (Jorgensen et al., 1985; Rink et al., 1998; Köhler-Rink and Kühl, 2000). Photosynthesis by the symbionts elevates the pH of the microenvironment (Jorgensen et al., 1985; Rink et al., 1998; Wolf-Gladrow et al., 1999; Köhler-Rink and Kühl, 2000), while calcification and respiration decrease it (Equation 2).

$$Ca^{2+} + 2HCO_3^- \leftrightarrow CaCO_3 + H_2O + CO_2 \leftrightarrow CaCO_3 + CH_2O + O_2 \quad (2)$$

The pH of the microenvironment the foraminifera is calcifying in, and thus the $\delta^{11}B$ should therefore reflect the relative dominance of these processes, which is hypothesized to covary with seawater pH and possibly cause the species-specific variation $\delta^{11}B$ deviations from $\delta^{11}B$ of borate ion. Theoretical predictions from Zeebe et al. (2003) and foraminiferal data from Hönisch et al., (2003) highlighted the dominance of microenvironment pH in $\delta^{11}B$ signature of foraminifera. Their work also suggested that for a given species, there should be a constant offset observed between the boron isotope composition of foraminifera and borate ion over a large range of pH, imparting confidence in utilizing species-specific boron isotope data as a proxy for seawater pH.

Comparison of boron isotope data for multiple planktonic foraminiferal species indicate that taxa with high levels of symbiont activity such as *T. sacculifer* and *G. ruber* show higher $\delta^{11}B$ values than the $\delta^{11}B$ of ambient borate (Foster et al., 2008, Henehan et al., 2013, Raitzsch et al., 2018). The sensitivities ($\Delta\delta^{11}B_{carbonate}/\Delta\delta^{11}B_{borate}$ referred to as the slope) of existing calibrations suggest a different species-specific sensitivity for these species compared to other taxa (Sanyal et al., 2001; Henehan et al., 2013; Henehan et al.,2015; Raitzsch et al., 2018). For example, *Orbulina universa* exhibits a lower $\delta^{11}B$ than *in situ* $\delta^{11}B$ values of borate ion (Henehan et al., 2016), consistent with the species living deeper in the water column characterized by reduced photosynthetic activity.

It is possible that photosynthetic activity by symbionts might not be able to compensate for changes in calcification and/or respiration, leading to an acidification of the microenvironment. It is interesting to note that for *O. universa* the slope determined for the field-collected samples is not statistically different from unity (0.95 ± 0.17) (Henehan et al. 2016), while culture experiments report slopes of ≤ 1 for multiple species including *G. ruber* (Henehan et al., 2013), *T. sacculifer* (Sanyal et al., 2001), and *O. universa* (Sanyal et al., 1999). More core-top and culture calibrations are needed to fully understand why different slopes are observed, which is part of the motivation for this study.

2.5 Planktic foraminifera depth and habitat preferences

The preferred depth habitat of different species of planktonic foraminifera depends on their ecology, which in turn relies on the hydrographic conditions. For example, *G. ruber is* commonly found in the mixed layer (Fairbanks and Wiebe, 1980; Dekens et al., 2002; Farmer et al., 2007) during the summer (Deuser et al., 1981) whereas *T. sacculifer* is present in the mixed layer until mid-thermocline depths (Farmer et al., 2007) during spring and summer (Deuser et al., 1981, 1989). Specimens of *P. obliquiloculata* and *N. dutertrei* are abundant during winter months (Deuser et al., 1989), with an acme in the mixed layer (~60m) for *P. obliquiloculata*, and at mid-thermocline depths for *N. dutertrei* (Farmer et al., 2007). In contrast, *O. universa* tends to record annual average conditions within the mixed layer. Specimens of *G .menardii* calcify within the seasonal thermocline (Fairbanks et al., 1982, Farmer et al., 2007, Regenberg et al., 2009), and in some regions in

https://doi.org/10.5194/bg-2019-266
Preprint. Discussion started: 8 August 2019

the upper thermocline (Farmer et al., 2007), and records annual temperatures. *G. tumida* is found at the lower thermocline or below the thermocline and records annual average conditions (Fairbanks and Wiebe, 1980; Farmer et al., 2007, Birch et al., 2013).

3. Materials and Methods

3.1 Localities studied

Core-top locations were selected to span a broad range of seawater pH, carbonate system parameters, and oceanic regimes. Samples from Atlantic Ocean (CD107-A), Indian Ocean (FC-01a and FC-02a), Arabian Sea (FC-13a and FC-12b) and Pacific Ocean (WP07-01, A14) were analyzed; characteristics of the sites are summarized in Table 1 and S7, Fig. 3, and Fig. 4.

Atlantic site CD107-a (CD107 site A) was drilled in 1997 by the Benthic Boundary Layer program (BENBO) (K.S. Black et al., 1997 - cruise report RRS Charles Darwin Cruise 107). Arabian Sea sites FC-12b (CD145 A150) and FC-13a (CD145 A3200) were retrieved by the *Charles Darwin* in the Pakistan Margin in 2004 (B.J. Bett et al., 2003 - cruise report n°50 RRS Charles Darwin Cruise 145). A14 was recovered by box corer in the southern area of the South China Sea in 2012. Core WP07-01 was obtained from the Ontong Java Plateau using a giant piston corer during the Warm Pool Subject Cruise in 1993.The top 10 cm of sediment from CD107-A have been radiocarbon dated to be Holocene <3 ky (Thomson et al., 2000). Samples from multiple box cores from Indian Ocean sites were radiocarbon dated as Holocene <7.3 ky (Wilson et al., 2012). Samples from western equatorial Pacific Site 806B, close to site WP07-01, are dated to between 7.3-8.6 ky (Lea et al., 2000). Arabian Sea and Pacific core-top samples were not radiocarbon dated but are assumed to be Holocene.

3.2 Species

Around 50-100 foraminifera shells were picked from the 400-500 µm fraction size for *Orbulina universa*, *Globorotalia menardii* and *Globorotalia tumida*, from the 300-400µm fraction size for *Trilobatus sacculifer* (w/o sacc, without sacc-like final chamber), *Trilobatus sacculifer* (sacc, sacc-like final chamber), *Neogloboquadrina dutertrei*, *Pulleniatina obliquiloculata* and from the 250-300 µm for *Globigerinoides ruber* (white, sensu stricto). The samples picked for analyses were visually well preserved.

3.3 Sample cleaning

Briefly, picked foraminifera were gently cracked open, clay removed and checked for coarse-grained silicates. The next stages of sample processing and chemical separation were performed in a class 1000 clean lab equipped with boron-free HEPA filters. Samples were then cleaned using full reductive and oxidative cleaning following Barker et al., (2003). A final leaching step with 0.001N HCl was done before dissolution in 1N HCl. Each sample was divided into two aliquots: an aliquot for boron purification and one aliquot for trace element analysis.

3.4 Reagents

Double-distilled HNO_3 and HCl acids (from Merck® grade) and a commercial bottle of HF Ultrapure grade were used at Brest. Double-distilled acids were used at Cambridge. All acids and further dilutions were prepared using double-distilled 18.2 MΩ.cm-1 MQ water. Working standards for isotope ratio and trace element

https://doi.org/10.5194/bg-2019-266
Preprint. Discussion started: 8 August 2019

measurements were freshly diluted on a daily basis with the same acids used for sample preparation to avoid any matrix effect.

32.5 Boron isotopes

Boron purification for isotopic measurement was done utilizing microdistillation method developed by Gaillardet et al., (2001), for Ca-rich matrices by Wang et al., (2010) and adapted at Cambridge by Misra et al., (2014a). 70 µL of dissolved carbonate sample was loaded on a cap of a clean fin legged 5 mL conical beaker upside down. The tightly closed beaker was put on a hotplate at 95°C for 15 hours. The beakers were taken off the hotplate and were allowed to cool for 15 min. The cap where the residue formed was replaced by a clean one. Then, 100 µL of 0.5% HF were added to the distillate.

Boron isotopic measurements were carried out on a Thermo Scientific ®Neptune+ MC-ICP-MS at the University of Cambridge. Neptune+ was equipped with Jet interface and two 10^{13} Ω resistors. The instrumental setup included Savillex® 50µl/min C-flow self-aspirating nebulizer, single pass Teflon® Scott-type spray chamber constructed utilizing Savillex® column components, 2.0 mm Pt injector from ESI®, Thermo® Ni 'H' type sample cone and 'X' type skimmer cones. Both isotopes of boron were determined utilizing 10^{13} Ω resistors (Misra et al., 2014a; Lloyd et al., 2018).

The sample size for boron isotope analyses typically ranged from 10 ppb B (~5 ng B) to 20 ppb B samples (~10 ng B). Instrumental sensitivity for ^{11}B was 17 mV/ppb B (eg. 170 mV for 10ppb B) in wet plasma at 50µl/min sample aspiration rate. Intensity of ^{11}B for a sample at 10ppb B was typically 165mV ± 5mV closely matched the 170mV ± 5mV of the standard. Due to the low boron content of the samples extreme care was taken to avoid boron contamination during sample preparation and reduce memory effect during analysis. Procedural boron blanks ranged from 15pg B to 65 pg B (contributed to less than <1% of the sample signal) and the acid blank during analyses was measured at ≤ 1mV on the ^{11}B, meaning a contribution < 1% of the sample intensity, no memory effect was observed within and across sessions.

Analyses of external standards were done to ensure data quality. For $\delta^{11}B$ measurements two carbonate standards were utilized: the JCP-1 (Geological Survey of Japan, Tsukuba, Japan) and the NEP internal coral standard (Porites sp., $\delta^{11}B$ = 26.12 ± 0.92 ‰, 2SD, n=33 Holcomb et al., 2015 and Sutton et al., 2018, Table S2) from University of Western Australia/Australian National University. Certified boron isotopes liquid standard, the ERM© AE121 ($\delta^{11}B$ = 19.9 ± 0.6 ‰, SD, certified) was used to monitor reproducibility and drift during each session (Vogl and Rosner, 2011; Foster et al., 2013; Misra et al., 2014). Results for the isotopic composition of the NEP standard are shown in Table S2, average values are $\delta^{11}B_{NEP}$ = 25.70 ± 0.93 ‰ (2SD, n=22) over different 7 analytical session with each number representing an ab-initio processed sample - this study). Our results are within error of published values of 26.20 ± 0.88‰ (2SD, n = 27) and 25.80 ± 0.89‰ (2SD, n = 6) by Holcomb et al. (2015) and Sutton et al. (2018) respectively. Chemically cleaned JCP_1 samples were measured at 24.06 ± 0.20 (2SD, n=6) and is within error of published values of 24.37 ± 0.32 ‰ and 24.42 ± 0.28 ‰ by Holcomb et al. (2015) and Sutton et al. (2018) respectively.

3.6 Trace elements

The calcium concentration of each sample was measured on an ICP-AES ® Ultima 2 HORIBA at the Pôle spectrometrie Océan (PSO), UMR6538 (Plouzané, France). Samples were then diluted to fixed calcium

https://doi.org/10.5194/bg-2019-266
Preprint. Discussion started: 8 August 2019

concentrations (typically 10 ppm or 30 ppm Ca) using 0.1 M HNO3 & 0.3 M HF matching multi-element standards Ca concentration to avoid any matrix effect (Misra et al., 2014b). Trace elements (e.g. X/Ca ratios) were analyzed on a Thermo Scientific ® Element XR HR-ICP-MS at the PSO, Ifremer (Plouzané, France).

Trace element analyses were done at a Ca concentration of 10 or 30 ppm. The typical blanks for a 30 ppm Ca session were: ^{7}Li < 2%, ^{11}B < 7%, ^{25}Mg < 0.2% and ^{43}Ca < 0.02%. Additionally, blanks for a 10 ppm Ca session were: ^{7}Li < 2.5%, ^{11}B < 10%, ^{25}Mg < 0.4% and ^{43}Ca < 0.05%. Due to strong memory effect for boron and instrumental drift on the Element XR, long sessions of conditioning were done prior analyses. Boron blanks were driven below 5% of signal intensity usually after 4 to 5 days of continuous analyses of carbonate samples. External reproducibility was determined on the consistency standard Cam-Wuellestorfi (courtesy of the University of Cambridge) (Misra et al., 2014b), Table S3. Our X/Ca ratio measurements on the external standard Cam-Wuellestorfi were all the time within error of the published value (Table S3) validating the robustness of our trace elements data. Analytical uncertainty of a single measurement was calculated from the reproducibility of the Cam-Wuellestorfi, measured during a particular mass spectrometry session. The analytical uncertainties on the X/Ca ratios are: 0.4 µmol/mol for Li/Ca, 7 µmol/mol for B/Ca and 0.01 mmol/mol for Mg/Ca (2SD, n=31) respectively.

3.7 Oxygen isotopes

Carbonate δ^{13}C and δ^{18}O were measured on a Gas Bench II coupled to a Delta V mass spectrometer at the stable isotope facility of Pôle spectrometrie Océan (PSO), Plouzané. Around 20 shells were weighed, crushed and clay removed. The recovered foraminifera were weighed in tubes and flushed with He gas. Samples were then digested in phosphoric acid and analyzed. Results were calibrated to the VPDB scale by international standard NBS19 and analytical precision on the in-house standard Ca21 was better than 0.11‰ for δ^{18}O (1SD, n=5) and 0.03‰ for δ^{13}C (1SD, n=5).

3.8 Calcification depth determination

We utilized two different chemo-stratigraphic methods to estimate the calcification depth in this study (Table 3 , S6 and S7). The first method, commonly used in paleoceanography, utilizes δ^{18}O measurements of the carbonate ($\delta^{18}O_c$) to estimate calcification depths (referred to as δ^{18}O-based calcification depths) (Schmidt et al., 2002; Mortyn et al., 2003; Sime et al., 2005; Farmer et al., 2007; Birsh et al., 2013). The second method utilizes Mg/Ca-based temperature estimates ($T_{Mg/Ca}$) to constrain calcification depths (Quintana Krupinski et al., 2017). In both cases, the postulate was that vertical profiles of seawater temperature are available for different seasons in ocean atlases and cruise reports, and that hydrographic data and geochemical proxy signatures can be compared to assess the depth in the water column that represents the species maximum abundance.

The two different methods to estimate calcification depth were then compared to published depth estimates for the basin, and where available, for the same site (Table S6). We chose literature values for calcification depths when available, or depths that were closest to what is known for the region or basin. As foraminifera migrate vertically in the water column, we applied (based on uncertainties of our measurements) an uncertainty of ±10m for calcification depths > 70 m and an uncertainty of ±20 m when calcification depths <70 m.

https://doi.org/10.5194/bg-2019-266
Preprint. Discussion started: 8 August 2019

3.9 $\delta^{11}B_{borate}$

Two of the carbonate system parameters are essential to calculate the entire suite of carbonate system. Following the approach of Foster et al., (2008) we used the GLODAP database (Key et al., 2004) corrected for anthropogenic inputs in order to estimate pre-industrial carbonate system parameters at each site. Temperature, salinity and pressure for each site are from the World ocean database 2013 (Boyer et al., 2013). We utilized the R© code in Henehan et al, (2016) (courtesy of Michael Henehan) to calculate the $\delta^{11}B_{borate}$ and derive our calibrations. Uncertainty for $\delta^{11}B_{borate}$ utilizing the code was similar to the one calculated by applying 2 standard deviations of the calculated $\delta^{11}B_{borate}$ within the limits imposed by the calcification depth.

The Matlab© template provided by Zeebe and Wolf-Gladow, (2001) was used to calculate pCO_2 from TA; temperature, salinity and pressure were included into the calculations. Total boron was calculated from Lee et al., (2010), K_1 and K_2 were calculated from Mehrbach et al. (1973) refitted by Dickson and Millero (1987).

Statistical tests were made utilizing GraphPad© software, linear regressions for calibration where derived utilizing R© code in Henehan et al, (2016) (courtesy of Michael Henehan) with a k=500.

4. Results

4.1 Depth habitat

The calcification depths utilized in this paper are summarized in Table S6, including a comparison of calcification depth determination methods. The calculated calcification depths are consistent with the ecology of each species and the hydrography of the sites. Specimens of *G. ruber* and *T. sacculifer* appear to be living in the shallow mixed layer, with *T. sacculifer* living or migrating deeper than *G. ruber*. Specimens of *O. universa* and *P. obliquiloculata* are living in the upper thermocline; *G. menardii* is found in the upper thermocline until the thermocline depth specific to the location; *N. dutertrei* is living around the thermocline depth and specimens of *G. tumida* are found in the lower thermocline.

Data from both approaches implies that some species inhabit deeper environments in the Western Equatorial Pacific (WEP) relative to the Arabian Sea, which in turn are deeper dwelling than in the Indian Ocean. In some cases, we find evidence for differences in habitat depth of up to ~100m between the WEP and the Arabian Sea. This trend is observed for *G. ruber* and *T. sacculifer*, but not for *O. universa*.

Some differences in calcification depth are observed between the two calcification depth determination methods. These differences might be due to the choice of calibrations. Alternatively our uncertainties for $\delta^{18}O$ implies larger uncertainties on the calcification depth determination using this approach, compared to Mg/Ca measurements.

4.2 Empirical calibrations of foraminiferal $\delta^{11}B_{carbonate}$ to $\delta^{11}B_{borate}$

Results for the different species analyzed in this study are presented in Fig. 5, Fig. 6 and summarized in Table 2; additionally, published calibrations for comparison are summarized in Table 3.

4.2.1 *G. ruber*

Our results for *G. ruber* (Fig. 5) are in good agreement with published data from other core-tops, sediment traps, tows, and culture experiments (Foster et al., 2008, Henehan et al., 2013, Raitzsch et al., 2018).

https://doi.org/10.5194/bg-2019-266
Preprint. Discussion started: 8 August 2019

Whilst this species has been widely studied previously, the sites selected in this study allow us to extend the calibration. The positive offset from the 1:1 curve has been explained by the high photosynthetic activity (Hönisch et al., 2003; Zeebe et al., 2003). The slope of our linear regression is not statistically different from 1 and do not follow the low sensitivity trend of the culture experiments from Sanyal et al., (2001) or Henehan et al., (2013), ($p<0.05$). Linear regression yields a slope of 1.12 ± 1.67, with a Y intercept of 1.23 ± 0.59 and a R^2 of 0.9762. The slope here is >1, implying a greater sensitivity of the $\delta^{11}B_{carbonate}$ to the $\delta^{11}B_{borate}$ than expected for this species.

4.2.2 *T. sacculifer*

$\delta^{11}B_{carbonate}$ results for *T. sacculifer* (sacc and w/o sacc) (Fig. 5) are compared to published data (Foster et al., 2008; Martinez-Boti et al., 2015, Raitzsch et al., 2018). Results for *T. sacculifer* are in good agreement with the literature and fall above the 1:1 line. Linear regression on our data yields a slope of 1.17 ± 2.11 but is not statistically different to the results from Martinez-Boti et al., (2015) (Table 3), ($p>0.05$). However when compiled with published data, a slope of 0.63 ± 0.56 is calculated, with a large uncertainty given the variability in the data. It is also noticeable that *T. sacculifer* (w/o sacc) samples from the WEP have a $\delta^{11}B_{carbonate}$ close to the 1:1 line.

4.2.3 Deeper dwelling species: *O. universa, N. dutertrei, P. obliquiloculata, G. menardii* and *G. tumida*

Our results for *O. universa* (Fig. 5), *N. dutertrei*, *P. obliquiloculata*, *G. menardii* and *G. tumida* (Fig. 6) fall below the 1:1 line. These data for *O. universa* are not statistically different from the Henehan et al. (2016) calibration ($p>0.05$). Our results for *N. dutertrei* expand upon the initial measurements presented in Foster et al., (2008). The different environments experienced by *N. dutertrei* in our study permit us to extend the range and derive a calibration for this species ($R^2=0.917$, $p=0.015$); the slope is close to unity (0.93 ± 0.55), and is similar to the (0.95 ± 0.17) previously reported by Henehan et al., (2016) for *O. universa* and not statistically different ($p>0.05$). The data for *P. obliquiloculata* exhibits the largest offset from the theoretical line. The range of $\delta^{11}B_{borate}$ from the samples we have of *G. menardii* and *G. tumida* is not sufficient to derive calibrations, but the points are in good agreement with the *N. dutertrei* calibration and Henehan et al. (2016) calibration for *O. universa*.

For all species, the slopes are not statistically different from Henehan et al. (2016) ($p>0.05$) and are close to unity. If data for deep-dwelling foraminiferal species are pooled together with each other and with data from Henehan et al., (2016) and Raitzch et al., (2018), we calculate a slope of 0.93 (± 0.13) ($R^2=0.7987$, $p<0.0001$); if only our data are used, we calculate a slope that is not significantly different (0.82 ± 0.27; $p<0.05$).. However, it may remain premature to assume that a unique calibration with a slope of ~0.9 can be used for all deeper-dwelling species; more data is needed for *P. obliquiloculata*, *G. menardii* and *G. tumida* to robustly test this assertion.

4.2.5 Comparison of coretop and culture data

The data for *G. ruber* and *T. sacculifer* from the coretops we measured are broadly consistent with previous published results. These taxa have symbionts that exhibit high photosynthetic activity and thus have calibrations higher than the 1:1 line. Notably, there is a difference in calibrations between these core-top derived

https://doi.org/10.5194/bg-2019-266
Preprint. Discussion started: 8 August 2019

estimates and culture experiments (Henehan et al., 2013; Marinez-Boti et al., 2015; Raitzsch et al., 2018; Table 3). This difference is particularly notable for *G. ruber*. Despite statistically different intercepts ($p<0.05$), the sensitivities of the species analyzed are not statistically different and are close to unity.

4.3 B/Ca ratios

B/Ca ratios are presented in Table 2. Values are species specific consistent with previous work (e.g., Yu et al., 2007; Henehan et al., 2015) with ratios higher for *G. ruber* > *T. sacculifer* > *T. sacculifer* (w/o sacc) > *P. obliquicloculata* >*N. dutertrei* > *O. universa* > *G. menardii* > *G. tumida* (Fig. S5). B/Ca differences between surface- and deep-dwelling foraminifera are observed, with lower values and a smaller range for the deeper dwelling taxa (58-126 µmol/mol vs 83-190 µmol/mol for shallow dwellers). The B/Ca data for deep-dwelling taxa exhibits a significant correlation with $[B(OH)_4^-]/[HCO_3^-]$ ($p>0.05$), but no correlation with $\delta^{11}B_{carbonate}$ and temperature (Fig. S4). Surface-dwelling species have B/Ca ratios that exhibit significant correlations with $[B(OH)_4^-]/[HCO_3^-]$, $\delta^{11}B_{carbonate}$ and temperature. The sensitivity of B/Ca to $[B(OH)_4^-]/[HCO_3^-]$ is lower for deep-dwelling species compared to surface dwelling species. When all the B/Ca data are compiled, significant trends are observed with $[B(OH)_4^-]/[HCO_3^-]$, $\delta^{11}B_{carbonate}$ and temperature (Fig. S4). We also observe that if we compare data from all sites together, correlations exist between B/Ca and the water depths of the cores (Fig. S5) but this correlation may be related to the different in the depth habitats of different taxa in each region.

5. Discussion

5.1 Sources of uncertainty relating to depth habitat and seasonality at studied sites

5.1.1 Depth habitats and $\delta^{11}B_{borate}$

Because foraminifera will record ambient environmental conditions during calcification, the accurate characterization of in-situ data is needed not only for calibrations, but also to understand the reconstructed record of pH or pCO_2. The species we examined are ordered here from shallower to deeper depth habitats: *G. ruber* >*T. sacculifer* (sacc) > *T. sacculifer* (w/o sac) > *O. universa* > *P. obliquiloculata* > *G. menardii* > *N. dutertrei* > *G. tumida* (this study; Birch et al., 2013; Farmer et al., 2007), although the specific water depth will vary depending on the hydrology of the site (Kemle-von and Oberhänhsli, 1999). We note that calculation of absolute calcification depths can be challenging in some cases as many species migrate during their ontogeny (Steinhardt et al., 2015). We find that assumptions about the specific depth habitat a species of foraminifera is calcifying over in a given region can lead to differences of a few per mil in calculated isotopic compositions of borate (Fig. 4).

Hence this can cause a bias in calibrations if calcification depths are assumed instead of being calculated (i.e., with $\delta^{18}O$ and/or Mg/Ca). At the sites we examined, most of the sampled species live in deeper depth habitats in the WEP relative to the Indian Ocean, which in turn is characterized by deeper depth habitats than in the Arabian Sea. In the tropical Pacific, *T. sacculifer* is usually found deeper than *G. ruber* except at sites characterized by a shallow thermocline, in which case they tend to overlap their habitat (e.g., ODP Site 806 in the WEP which has a deeper thermocline than at ODP Site 847 in the Eastern Equatorial Pacific; EEP) (Rickaby

https://doi.org/10.5194/bg-2019-266
Preprint. Discussion started: 8 August 2019

462 et al., 2005). The difference in depth habitats for *T. sacculifer* and *N. dutertrei* between the WEP and EEP can be
463 as much as almost 100 m (Rickaby et al., 2005).
464
465 **5.1.2 Seasonality and in-situ $\delta^{11}B_{borate}$**
466 As discussed by Raitzsch et al., (2018), depending of the study area, foraminiferal fluxes can change
467 throughout the year, so seasonality can have a major impact on hydrographic carbonate parameters calculations
468 for any given water depth. We therefore recalculated the theoretical $\delta^{11}B_{borate}$ using seasonal data for temperature
469 and salinity and annual values for TA and DIC for each depth at each site. The GLODAP (2013) database does
470 not provide seasonal TA or DIC values.
471 The low sensitivity of $\delta^{11}B_{borate}$ to temperature and salinity means that calculated $\delta^{11}B_{borate}$ for each
472 water depth at our sites were not strongly impacted (Fig. S1). Thus, these findings support Raitzsch et al. (2018),
473 who concluded that calculated $\delta^{11}B_{borate}$ values corrected for seasonality was within error of non-corrected values
474 for each water depth. As Raitzsch et al, (2018) highlight, seasonality might be more important at high latitude
475 sites where seasonality is more marked.
476 Data for our sites suggests that most $\delta^{11}B_{borate}$ variability we observe does not come from seasonality but
477 from the assumed water depths for calcification. With the exception of a few specific area such as the Red Sea
478 (Henehan et al., 2016, Raitzsch et al., 2018), at most sites examined, seasonal $\delta^{11}B_{borate}$ does not vary by more
479 than ~0.2‰. We conclude that seasonality is not an important factor impacting carbonate system parameters at
480 the sites we examined.
481
482 **5.2 $\delta^{11}B$, microenvironment pH and depth habitats**
483 It is now accepted that the $\delta^{11}B$ signature comes from the microenvironment pH (Jorgensen et al., 1985;
484 Rink et al., 1998; Köhler-Rink and Kühl, 2000, Hönisch et al., 2003; Zeebe et el., 2003). Foraminifera with high
485 photosynthetic activity like *G.ruber* and *T. sacculifer* present a pH of microenvironment higher than ambient
486 seawater, $\delta^{11}B$ higher than 1:1 line (Foster et al., 2008, Henehan et al., 2013, Raitzsch et al., 2018). The opposite
487 is also true, species with weaker photosynthetic activity present microenvironments lower than ambient
488 seawater, $\delta^{11}B$ lower than 1:1 line (Martinez-Boti et al., 2015; Henehan et al., 2016), this is the case in our data
489 for *O. universa*, *N. dutertrei*, *G. tumida*, *G. menardii* and *P. obliquiloculata*.
490 The photosynthetic activity is directly a function of the light level they received which is in the natural
491 system dependent of their depth in the water column. In this case, the photosynthetically active foraminifera
492 living close to the surface should see their microenvironment pH (thus $\delta^{11}B$) more sensitive to water depth
493 changes. A deeper depth habitat will change the light intensity they received and as a consequence may lower
494 their photosynthetic activity reducing their microenvironment pH. This thought is supported by the significant
495 trend observed between our $\Delta^{11}B$ and the calcification depth for *G. ruber* and *T. sacculifer* of our sites (Fig. S2).
496 This trend basically supports the fact that the microenvironment pH decrease with calcification depth.
497 Especially, we observe an important decrease of $\delta^{11}B$ in the WEP for *T. sacculifer (w/o sacc)*. To test if the $\delta^{11}B$
498 signature was inferred to a light driven, we have been able to independently calculate the depth of the
499 foraminifera based on various light insolation culture experiments (Jorgensen et al., 1985) and the
500 microenvironment pH derived from our data (Fig. S3). This exercise verified that this low $\delta^{11}B$ can be explained
501 by the reduced light environment due to a deeper depth habitat in the WEP (Fig. 7). When applied to our *O.*

https://doi.org/10.5194/bg-2019-266
Preprint. Discussion started: 8 August 2019

universa data suggest a microenvironment pH 0.10 to 0.20 lower than ambient seawater pH which would be in line with species living deeper than 50m (light compensation point (Ec), Rink et al., 1998) also consistent with our calcification depth reconstructions. Also, the higher $\delta^{11}B$ data from the African upwelling published by Raitzsch et al., (2018) for *G. ruber* and *O. universa* might reflect the higher microenvironment pH due to a shallower depth habitat. This could highlight a potential issue with calibration when applied to sites with different oceanic regimes as the $\delta^{11}B$ specie-specific calibrations could be also location-specific for the mixed dweller species.

Microenvironment pH results for *N. dutertrei*, *G. menardii*, *G. tumida*, are similar to *O. universa* and suggest a threshold for respiration driven $\delta^{11}B$ signature. This threshold especially makes sense as not all the species are symbiont bearing (eg. *O. universa*, *G. ruber*, *T. sacculifer*), but they can be symbiont facultative, this is the case for *N. dutertrei*, *G. menardii*, *P. obliquiloculata* (Hembleden et al., 1979). We can explain this threshold because deep dweller species do not experience important changes of insolation at those depths so their microenvironments should be respiration driven and relatively stable.

5.3 $\delta^{11}B$ sensitivity to $\delta^{11}B_{borate}$ and relationship with B/Ca signatures

$\delta^{11}B_{carbonate}$ and B/Ca data have shown to be sensitive to precipitation rate with at higher precipitation rate increasing $\delta^{11}B_{carbonate}$ (Farmer et al., 2019) and B/Ca (Farmer et al., 2019; Gabitov et al., 2014; Kaczmarek et al., 2016 ; Mavromatis et al., 2015; Ushikawa et al., 2015). A recent study from Farmer et al, (2019) has proposed that in foraminifera at higher precipitation rates, more borate ion is incorporated into the carbonate mineral, while at lower precipitation rates, more boric acid is incorporated. They also suggest this may explain low sensitivities of culture experiments.

The observation that slopes are not statistically different from unity for most of the species investigated implies that for these taxa, changes in precipitation rate and contributions of boric acid are not likely to be important. The higher values for *G. ruber* (1.12 ± 1.67) and *T. sacculifer* (1.17± 2.11), however, mean that the observed high values for $\delta^{11}B_{carbonate}$ at high seawater pH might be due to higher precipitation rates. We note this would also be consistent with the higher sensitivity of B/Ca signatures in these two surface dwelling species to ambient $[B(OH)_4^-]/[HCO_3^-]$ relative to deeper dwelling species. As indicated by Farmer et al., (2019), studies of calcite precipitation rates in foraminifera could help to test this hypothesis and improve our understanding of the fundamental basis of boron-based proxies.

5.4 Evaluation of species for pH reconstructions and water depth pH reconstructions

This data set allows us to reassess the utility of boron based proxies for the carbonate system. The main interest with utilizing boron-based proxies relates to the reconstruction of past oceanic conditions - specifically pH and pCO_2. Mixed-layer species (eg. *G. ruber* and *T. sacculifer)* are potential archives for atmospheric CO_2 reconstructions. Other species can shed light on other aspects of the carbon cycle including the biological pump.

There are a few main inferences we can make. First, our results highlight a potential mismatch between field-collected samples and culture studies, and support the observations of Henehan et al., (2016) for *O. universa*. In order to derive accurate reconstructions of past ambient pH and pCO_2, accurate species-specific calibrations need to be used that are constrained by core-tops or samples from similar types of settings (Fig. 9,

https://doi.org/10.5194/bg-2019-266
Preprint. Discussion started: 8 August 2019

10, S6). Lighter $\delta^{11}B$ signatures in *T. sacculifer* (w/o sacc) and *G. ruber* are observed in the WEP, which is likely explained by the deeper depth habitat for these taxa in the WEP leading to a lower light levels.

We also find that for four species, the boron proxy is a relatively straightforward recorder of ambient pH, with sensitivities close to unity for *G. ruber*, *T. sacculifer*, *O. universa*, *and N. dutertrei*. There is also promise in using multiple species in a sample from different hydrographic regimes to reconstruct vertical profiles of pH and pCO_2. We are able to reproduce pH and pCO_2 profiles from multiple sites with different water column structures (Fig. 9) with those reconstructions within error of the in-situ values, for most sites. In order to check our calibrations, we recalculated ambient pH and pCO_2 using our derived calibrations. We utilized the calibrations derived from our data for *G. ruber* (calibration n°2, Table 3), *T. sacculifer* (calibration n°1, Table 3), *O. universa* (calibration n°7, Table 3), for *P. obliquiloculata* (calibration n°10, Table 3), and for *N. dutertrei*, *G. tumida* and *G. menardii* the calibration made on the compilation of the deep-dweller (calibration 12, Table 3). Results are shown in Fig. 9 and evaluated in Fig. 10. For *G. menardii*, more data would be helpful to provide additional constraints.

6. Conclusions and future implications

Our study has extended the boron isotope proxy with data for new species and sites. The work supports previous work showing that depth habitats of foraminifera vary depending on the oceanic regime, and this impacts boron isotope signatures. Low $\delta^{11}B$ values in the WEP compared to other regions for *T. sacculifer* (w/o sacc) may be explained by a reduction in microenvironment pH due to a deeper depth habitat associated with reduced irradiance and thus photosynthetic activity. Those results might also highlight a potential need for studying core-tops in order to establish what factors are important to accurately develop reconstructions in different areas.

The sensitivity of $\delta^{11}B$ to pH is not statistically different from unity for *G. ruber*, *O. universa* and *N. dutertrei*. *G. menardii* and *G. tumida* are similar to other deep-dwellers but more data are needed to fully determine their $\delta^{11}B$ sensitivities to pH. The similarity of boron isotope calibrations for deep-dwelling taxa might be related to respiration-driven microenvironments.

Reconstruction of seawater pH and carbonate system parameters is achievable using foraminiferal $\delta^{11}B$. Past pH and pCO_2 water depth profiles can potentially be created by utilizing multiple foraminiferal species in concert with taxon-specific calibrations for similar settings. This approach has much potential for enhancing our understanding of the past workings of the oceanic carbon cycle, and the biological pump.

https://doi.org/10.5194/bg-2019-266
Preprint. Discussion started: 8 August 2019

Author contribution

A.T. and R.E wrote the proposals that funded the work. A.T. and F.C. provided the samples. M.G., S.M. and A.T. contributed to the experimental design. A.V. helped for sample preparation. M.G. and S.M contributed to developing the method of boron isotope analysis. M.G. performed the measurements with assistance from S.M. M.G conducted the data analysis. M.G. drafted the paper, which was edited by all authors. Interpretation was led by M.G., A.T., S.M. with input from R.E., A.V. and F.C.

Competing interests

The authors declare that they have no conflict of interest.

Acknowledgments:

The authors wish to thank Lea Bonnin for assistance with picking samples, the IODP repository for provision of samples, the Tripati Laboratory (UCLA) for their technical support, Mervyn Greaves, Madeleine Bohlin (University of Cambridge) for technical support and use of laboratory space, Yoan Germain, Emmanuel Ponzevera and Oanez Lebeau for technical support and use of laboratory space in Brest, Jill Sutton for helpful conversation on the manuscript. Jesse Farmer and two anonym reviewers provided helpful reviews on a previous version of this manuscript. Research is supported by the International Research Chair Program that is funded by the French government (LabexMer ANR-10-LABX-19-01), DOE BES grant DE-FG02-13ER16402 and IAGC student research grant 2017.

https://doi.org/10.5194/bg-2019-266
Preprint. Discussion started: 8 August 2019

592 **References**

593 Allen, K. A. and Hönisch, B.: The planktic foraminiferal B/Ca proxy for seawater carbonate chemistry: A critical
594 evaluation, Earth Planet. Sci. Lett, 345–348, 203–211, 2012.

595 Anand, P., Elderfield, H. and Conte, M. H.: Calibration of Mg/Ca thermometry in planktonic foraminifera from a
596 sediment trap time series. Paleoceanography 18, 2003.

597 Arbuszewski, J., DeMenocal, P., Kaplan, A. and Farmer, E. C.: On the fidelity of shell-derived δ18Oseawater
598 estimates, Earth Planet. Sci. Lett., 300, 185–196, 2010.

599 Axelsson, M. D., Rodushkin, I., Ingri, J. and Öhlander, B.: Multielemental analysis of Mn–Fe nodules by ICP-
600 MS: optimisation of analytical method, Analyst, 127, 76–82, 2002.

601 Barker S., Greaves M. and Elderfield H.: A study of cleaning procedures used for foraminiferal Mg/Ca
602 paleothermometry. Geochemistry, Geophys. Geosystems 4, 1–20, 2003.

603 Bartoli, G., Hönisch, B. and Zeebe, R. E.: Atmospheric CO2 decline during the Pliocene intensification of
604 Northern Hemisphere glaciations. Paleoceanography 26, 1–14, 2011.

605 Bemis, B. E., Spero, H. J., Bijma, J. and Lea, D. W.: Reevaluation of the oxygen isotopic composition of
606 planktonic foraminifera: Experimental results and revised paleotemperature equations. Paleoceanography
607 13, 150–160, 1998.

608 Bemis, B. E., Spero, H. J. and Thunell, R. C.: Using species-specific paleotemperature equations with
609 foraminifera: a case study in the Southern California Bight, Mar. Micropaleontol, 46, 405–430, 2002.

610 Bijma, J., Faber Jr., W.W., Hemleben, C.: Temperature and salinity limits for growth and survival of some
611 planktonic foraminifers in laboratory cultures, J. Foraminiferal Res. 20 (2), 95–116, 1990.

612 Bijma, J., Hönisch, B. and Zeebe, R. E.: Impact of the ocean carbonate chemistry on living foraminiferal shell
613 weight: Comment on "Carbonate ion concentration in glacial-age deep waters of the Caribbean Sea" by W.
614 S. Broecker and E. Clark, Geochemistry, Geophys. Geosystems, 3, 1–7, 2002.

615 Birch, H., Coxall, H. K., Pearson, P. N., Kroon, D. and O'Regan, M.: Planktonic foraminifera stable isotopes and
616 water column structure: Disentangling ecological signals, Mar. Micropaleontol., 101, 127–145, 2013.

617 Boyer, T.P., Antonov, J. I., Baranova, O. K., Coleman, C., Garcia, H. E., Grodsky, A., Johnson, D. R., Locarnini,
618 R. A., Mishonov, A. V., O'Brien, T.D., Paver, C.R., Reagan, J.R., Seidov, D., Smolyar, I. V., and Zweng,
619 M. M.: World Ocean Database, NOAA Atlas NESDIS 72, S. Levitus, Ed., A. Mishonov, Technical Ed.,
620 Silver Spring, MD, 209, 2013.

621 Boyle, E. A.: Manganese carbonate overgrowths on foraminifera tests, Geochim. Cosmochim. Acta., 47, 1815–
622 1819, 1983.

623 Branson, O., Kaczmarek, K., Redfern, S. A. T., Misra, S., Langer, G., Tyliszczak, T., Bijma, J. and Elderfield,
624 H.: The coordination and distribution of B in foraminiferal calcite, Earth Planet. Sci. Lett., 416, 67–72,
625 2015.

626 Catanzaro, E.J., Champion, C.E., Garner, A.L., Marinenko, G., Sappenfield, K.M. and Shields, W.R.: Boric
627 Acid; Isotopic and Assay Standard Reference Materials. U.S. Natl. Bur. Stand. Spec., Publ. 260-17, 70p,
628 1970.

629 Chalk, T. B., Hain, M. P., Foster, G. L., Rohling, E. J., Sexton, P. F., Badger, M. P. S., Cherry, S. G., Hasenfratz,
630 A. P., Haug, G. H., Jaccard, S. L., Martínez-García, A., Pälike, H., Pancost, R. D. and Wilson, P. A.:

https://doi.org/10.5194/bg-2019-266
Preprint. Discussion started: 8 August 2019

631 Causes of ice age intensification across the Mid-Pleistocene Transition, Proc. Natl. Acad. Sci., 114,
632 13114–13119, 2017.

633 Coadic, R., Bassinot, F., Dissard, D., Douville, E., Greaves, M. and Michel, E.: A core-top study of dissolution
634 effect on B/Ca in Globigerinoides sacculifer from the tropical Atlantic: Potential bias for paleo-
635 reconstruction of seawater carbonate chemistry, Geochemistry, Geophys. Geosystems 14, 1053–1068,
636 2013.

637 de Nooijer, L. J., Spero, H. J., Erez, J., Bijma, J. and Reichart, G. J.: Biomineralization in perforate foraminifera.
638 Earth-Science Rev., 135, 48–58, 2014.

639 Dekens, P. S., Lea, D. W., Pak, D. K. and Spero, H. J.: Core top calibration of Mg/Ca in tropical foraminifera:
640 Refining paleotemperature estimation, Geochemistry, Geophys. Geosystems 3, 1–29, 2002.

641 Deuser, W.G., Ross, E.H., Hemleben, Ch., Spindler, M.: Seasonal changes in species composition, numbers,
642 mass, size, and isotopic composition of planktonic foraminifera settling into the deep Sargasso Sea,
643 Palaeogeogr., Palaeoclimat., Palaeoecol., 33:103-127, 1981.

644 Deuser, W. G. and Ross, E. H.: Seasonally abundant planktonic foraminifera of the Sargasso Sea; succession,
645 deep-water fluxes, isotopic compositions, and paleoceanographic implications, J. Foraminifer. Res. 19,
646 268–293, 1989.

647 Dickson, A. G.: Thermodynamics of the dissociation of boric acid in synthetic seawater from 273.15 to 318.15
648 K., Deep Sea Res., Part A, Oceanogr. Res. Pap. 37, 755–766, 1990.

649 Dickson, A.G., Millero, F.J.: A comparison of the equilibrium constants for the dissociation of carbonic acid in
650 seawater media, Deep-Sea Res., 34, 1733–1743, 1987.

651 Douville, E., Paterne, M., Cabioch, G., Louvat, P., Gaillardet, J., Juillet-Leclerc, A. and Ayliffe, L.: Abrupt sea
652 surface pH change at the end of the Younger Dryas in the central sub-equatorial Pacific inferred from
653 boron isotope abundance in corals (Porites), Biogeosciences 7, 2445–2459, 2010.

654 Duplessy, J., Labeyrie, L., Juilletleclerc, A., Maitre, F., Duprat, J. and Sarnthein, M.: Surface salinity
655 reconstruction of the north-atlantic ocean during the last glacial maximum, Oceanol. Acta, 14, 311–324,
656 1991.

657 Elderfield, H., Yu, J., Anand, P., Kiefer, T. and Nyland, B.: Calibrations for benthic foraminiferal Mg/Ca
658 paleothermometry and the carbonate ion hypothesis, Earth Planet. Sci. Lett., 250, 633–649., 2006.

659 Elderfield, H. and Granssen, G.: Past temperatures and O18 of surface ocean waters inferred from foraminiferal
660 Mg/Ca ratios, Nature 405, 442–445, 2000.

661 Erez, J.: The Source of Ions for Biomineralization in Foraminifera and Their Implications for Paleoceanographic
662 Proxies, Rev. Mineral. Geochemistry, 54, 115–149, 2003.

663 Fairbanks, R. G. and Wiebe, P. H.: Foraminifera and Chlorophyll Maximum: Vertical Distribution, Seasonal
664 Succession, and Paleoceanographic Significance, Science, 209, 1524–1526, 1980.

665 Fairbanks, R. G., Sverdlove, M., Free, R., Wiebe, P. H. and Bé, A. W. H.: Vertical distribution and isotopic
666 fractionation of living planktonic foraminifera from the Panama Basin, Nature, 298, 841–844, 1982.

667 Farmer, E. C., Kaplan, A., de Menocal, P. B. and Lynch-Stieglitz, J.: Corroborating ecological depth preferences
668 of planktonic foraminifera in the tropical Atlantic with the stable oxygen isotope ratios of core top
669 specimens, Paleoceanography, 22, 1–14, 2007.

670 Feely, R.: Impact of Anthropogenic CO2 on the CaCO3 System in the Oceans, Science, 305, 362–366, 2004.

https://doi.org/10.5194/bg-2019-266
Preprint. Discussion started: 8 August 2019

Ferguson, J. E., Henderson, G. M., Kucera, M. and Rickaby, R. E. M.: Systematic change of foraminiferal Mg/Ca ratios across a strong salinity gradient, Earth Planet. Sci. Lett., 265, 153–166, 2008.

Foster, G. L.: Seawater pH, pCO2 and [CO32−] variations in the Caribbean Sea over the last 130 kyr: A boron isotope and B/Ca study of planktic foraminifera, Earth Planet. Sci. Lett., 271, 254–266, 2008.

Foster, G. L. and Sexton, P. F.: Enhanced carbon dioxide outgassing from the eastern equatorial Atlantic during the last glacial, Geology, 42, 1003–1006, 2014.

Foster, G. L., Lear, C. H. and Rae, J. W. B.: The evolution of pCO2, ice volume and climate during the middle Miocene, Earth Planet. Sci. Lett., 341–344, 243–254, 2012.

Foster, G. L. and Rae, J. W. B.: Reconstructing Ocean pH with Boron Isotopes in Foraminifera, Annu. Rev. Earth Planet. Sci., 44, 207–237, 2016.

Gabitov, R. I., Rollion-bard, C., Tripati, A. and Sadekov, A.: In situ study of boron partitioning between calcite and fluid at different crystal growth rates, Geochim. Cosmochim. Acta, 137, 81–92, 2014.

Gaillardet, J., Lemarchand, D., Göpel, C. and Manhès, G.: Evaporation and Sublimation of Boric Acid : Application for Boron Purification from Organic Rich Solutions, Geostand. Newsl., 25, 67–75, 2001.

Gattuso, J.P. and Hansson, L.: Ocean acidification, Oxford University Press, 2011.

Hemming, N. G. and Hanson, G. N. Boron isotopic composition and concentration in modern marine carbonates, Geochim. Cosmochim. Acta, 56, 537–543, 1992.

Henehan, M. J., Foster, G. L., Bostock, H. C., Greenop, R., Marshall, B. J. and Wilson, P. A.: A new boron isotope-pH calibration for Orbulina universa, with implications for understanding and accounting for 'vital effects', Earth Planet. Sci. Lett., 454, 282–292, 2016.

Henehan, M. J., Foster, G. L., Rae, J. W. B., Prentice, K. C., Erez, J., Bostock, H. C., Marshall, B. J. and Wilson, P. A.: Evaluating the utility of B/Ca ratios in planktic foraminifera as a proxy for the carbonate system: A case study of Globigerinoides ruber, Geochemistry, Geophys. Geosystems 16, 1052–1069, 2015.

Henehan, M. J., Rae, J. W. B., Foster, G. L., Erez, J., Prentice, K. C., Kucera, M., Bostock, H. C., Martínez-Botí, M. A., Milton, J. A., Wilson, P. A., Marshall, B. J. and Elliott, T.: Calibration of the boron isotope proxy in the planktonic foraminifera Globigerinoides ruber for use in palaeo-CO2reconstruction, Earth Planet. Sci. Lett. 364, 111–122, 2013.

Holcomb, M., Decarlo, T. M., Schoepf, V., Dissard, D., Tanaka, K. and McCulloch, M.: Cleaning and pre-treatment procedures for biogenic and synthetic calcium carbonate powders for determination of elemental and boron isotopic compositions, Chem. Geol., 398, 11–21, 2015.

Hönisch, B., Hemming, N. G., Archer, D., Siddall, M. and McManus, J. F.: Atmospheric Carbon Dioxide Concentration Across the Mid-Pleistocene Transition, Science, 324, 1551–1554, 2009.

Hönisch, B., Bijma, J., Russell, A. D., Spero, H. J., Palmer, M. R., Zeebe, R. E. and Eisenhauer, A.: The influence of symbiont photosynthesis on the boron isotopic composition of foraminifera shells, Mar. Micropaleontol., 49, 87–96, 2003.

Hönisch, B. and Hemming, N. G.: Ground-truthing the boron isotope-paleo-pH proxy in planktonic foraminifera shells: Partial dissolution and shell size effects, Paleoceanography 19, 1–13, 2004.

Hönisch, B., Bickert, T. and Hemming, N. G.: Modern and Pleistocene boron isotope composition of the benthic foraminifer Cibicidoides wuellerstorfi, Earth Planet. Sci. Lett., 272, 309–318, 2008.

https://doi.org/10.5194/bg-2019-266
Preprint. Discussion started: 8 August 2019

Howes, E. L., Kaczmarek, K., Raitzsch, M., Mewes, A., Bijma, N., Horn, I., Misra, S., Gattuso, J. P. and Bijma, J.: Decoupled carbonate chemistry controls on the incorporation of boron into Orbulina universa, Biogeosciences, 14, 415–430, 2017.

IPCC: Climate Change 2014 - The Physical Science Basis, edited by Intergovernmental Panel on Climate Change, Cambridge University Press, Cambridge., 2014.

Jørgensen, B. B., Erez, J., Revsbech, P. and Cohen, Y.: Symbiotic photosynthesis in a planktonic foraminifera, Globigerinoides sacculifer (Brady), studied with microelectrodes, Limnol. Oceanogr., 30, 1253–1267 1985.

Kaczmarek, K., Nehrke, G., Misra, S., Bijma, J. and Elderfield, H.: Investigating the effects of growth rate and temperature on the B/Ca ratio and δ11B during inorganic calcite formation, Chem. Geol., 421, 81–92, 2016.

Kemle-von Mücke S. and Oberhänsli H.: The Distribution of Living Planktic Foraminifera in Relation to Southeast Atlantic Oceanography, Use Proxies Paleoceanogr., 91–115, 1999.

Key, R.M.: A global ocean carbon climatology: Results from Global Data Analysis Project (GLODAP), Global Biogeochem. Cycles, 18, GB4031, 2004.

Kim, S.-T. and O'Neil, J. R.: Equilibrium and nonequilibrium oxygen isotope effects in synthetic carbonates, Geochim. Cosmochim. Acta, 61, 3461–3475, 1997.

Klochko, K., Cody, G. D., Tossell, J. A., Dera, P. and Kaufman, A. J.: Re-evaluating boron speciation in biogenic calcite and aragonite using 11B MAS NMR, Geochim. Cosmochim. Acta, 73, 1890–1900, 2009.

Klochko, K., Kaufman, A. J., Yao, W., Byrne, R. H. and Tossell, J. A.: Experimental measurement of boron isotope fractionation in seawater, Earth Planet. Sci. Lett., 248, 276–285, 2006.

Köhler-Rink, S. and Kühl, M.: Microsensor studies of photosynthesis and respiration in larger symbiotic foraminifera. I. The physico-chemical microenvironment of Marginopora vertebralis, Amphistegina lobifera and Amphisorus hemrichii, Mar. Biol., 137, 473–486, 2000.

Köhler-Rink, S. and Kühl, M., Microsensor studies of photosynthesis and respiration in the larger symbiont bearing foraminifera Amphistegina lobifera, and Amphisorus hemprichii, Ophelia, 55, 111–122, 2001.

Lea, D. W., Pak, D. K. and Spero, H. J.: Climate impact of late quaternary equatorial Pacific sea surface temperature variations, Science, 289, 1719–1724, 2000.

Lemarchand, D., Gaillardet, J., Lewin, A. and Allègre, C. J.: Boron isotope systematics in large rivers: Implications for the marine boron budget and paleo-pH reconstruction over the Cenozoic, Chem. Geol., 190, 123–14, 2002.

Liu, Y., Liu, W., Peng, Z., Xiao, Y., Wei, G., Sun, W., He, J., Liu, G. and Chou, C.-L.: Instability of seawater pH in the South China Sea during the mid-late Holocene: Evidence from boron isotopic composition of corals, Geochim. Cosmochim. Acta, 73, 1264–1272, 2009.

Lloyd, N. S., Sadekov, A. Y. and Misra, S.: Application of 1013ohm Faraday cup current amplifiers for boron isotopic analyses by solution mode and laser ablation multicollector inductively coupled plasma mass spectrometry, Rapid Commun. Mass Spectrom., 32, 9–18, 2018.

Martínez-Botí, M. A., Foster, G. L., Chalk, T. B., Rohling, E. J., Sexton, P. F., Lunt, D. J., Pancost, R. D., Badger, M. P. S. and Schmidt, D. N.: Plio-Pleistocene climate sensitivity evaluated using high-resolution CO2 records, Nature, 518, 49–54, 2015.

https://doi.org/10.5194/bg-2019-266
Preprint. Discussion started: 8 August 2019

750 Martínez-Botí, M. A., Mortyn, P. G., Schmidt, D. N., Vance, D. and Field, D. B.: Mg/Ca in foraminifera from
751 plankton tows: Evaluation of proxy controls and comparison with core tops, Earth Planet. Sci. Lett., 307,
752 113–125, 2011.

753 Mavromatis, V., Montouillout, V., Noireaux, J., Gaillardet, J. and Schott, J.: Characterization of boron
754 incorporation and speciation in calcite and aragonite from co-precipitation experiments under controlled
755 pH, temperature and precipitation rate, Geochim. Cosmochim. Acta, 150, 299–313, 2015.

756 McCulloch, M. T., D'Olivo, J. P., Falter, J. L., Georgiou, L., Holcomb, M., Montagna, P. and Trotter, J. A.
757 Boron Isotopic Systematics in Scleractinian Corals and the Role of pH Up-regulation, Boron Isot. Adv.
758 Isot. Geochemistry, 2018.

759 Millero, F.: Speciation of metals in natural waters, Geochem. Trans., 2, 57, 2001.

760 Millero, F., Woosley, R., DiTrolio, B. and Waters, J.: Effect of Ocean Acidification on the Speciation of Metals
761 in Seawater, Oceanography 22, 72–85, 2009.

762 Misra, S., Greaves, M., Owen, R., Kerr, J., Elmore, A. C. and Elderfield, H.: Determination of B/Ca of natural
763 carbonates by HR-ICP-MS, Geochemistry, Geophys. Geosystems, 15, 1617–1628, 2014a.

764 Misra, S., Owen, R., Kerr, J., Greaves, M. and Elderfield, H.: Determination of δ11B by HR-ICP-MS from mass
765 limited samples: Application to natural carbonates and water samples, Geochim. Cosmochim. Acta, 140,
766 531–552, 2014b.

767 Mortyn, P. G. and Charles, C. D.: Planktonic foraminiferal depth habitat and δ 18 O calibrations: Plankton tow
768 results from the Atlantic sector of the Southern Ocean, Paleoceanography, 18, 2003.

769 Mulitza, S., Boltovskoy, D., Donner, B., Meggers, H., Paul, A. and Wefer, G.: Temperature:δ18O relationships
770 of planktonic foraminifera collected from surface waters, Palaeogeogr. Palaeoclimatol. Palaeoecol., 202,
771 143–152, 2003.

772 Ni, Y., Foster, G. L., Bailey, T., Elliott, T., Schmidt, D. N., Pearson, P., Haley, B. and Coath, C.: A core top
773 assessment of proxies for the ocean carbonate system in surface-dwelling foraminifers, Paleoceanography
774 22, 2007.

775 Nir, O., Vengosh, A., Harkness, J. S., Dwyer, G. S. and Lahav, O.: Direct measurement of the boron isotope
776 fractionation factor: Reducing the uncertainty in reconstructing ocean paleo-pH, Earth Planet. Sci. Lett.,
777 414, 1–5, 2015.

778 Noireaux, J., Mavromatis, V., Gaillardet, J., Schott, J., Montouillout, V., Louvat, P., Rollion-Bard, C. and
779 Neuville, D. R.: Crystallographic control on the boron isotope paleo-pH proxy, Earth Planet. Sci. Lett.,
780 430, 398–407, 2015.

781 Orr, J. C., Fabry, V. J., Aumont, O., Bopp, L., Doney, S. C., Feely, R. A., Gnanadesikan, A., Gruber, N., Ishida,
782 A., Joos, F., Key, R. M., Lindsay, K., Maier-Reimer, E., Matear, R., Monfray, P., Mouchet, A., Najjar, R.
783 G., Plattner, G. K., Rodgers, K. B., Sabine, C. L., Sarmiento, J. L., Schlitzer, R., Slater, R. D., Totterdell, I.
784 J., Weirig, M. F., Yamanaka, Y. and Yool, A.: Anthropogenic ocean acidification over the twenty-first
785 century and its impact on calcifying organisms, Nature, 437, 681–686, 2005.

786 Pagani. M.: Marked Decline in Atmospheric Carbon Dioxide Concentrations During the Paleogene, Science,
787 309, 600–603, 2005.

788 Palmer, M. R., Pearson, P. N. and Cobb, S. J., Reconstructing Past Ocean pH-Depth Profiles, Science, 282,
789 1468–1471, 1998.

790 Pearson, P. N. and Palmer, M. R.: Middle Eocene seawater pH and atmospheric carbon dioxide concentrations,
791 Science, 284, 1824–1826, 1999.

https://doi.org/10.5194/bg-2019-266
Preprint. Discussion started: 8 August 2019

792 Peeters, F. J. C. and Brummer, G.-J. a.: The seasonal and vertical distribution of living planktic foraminifera in
793 the NW Arabian Sea, Geol. Soc. London, Spec. Publ., 195, 463–497, 2002.

794 Quintana Krupinski, N. B., Russell, A. D., Pak, D. K. and Paytan, A.: Core-top calibration of B/Ca in Pacific
795 Ocean Neogloboquadrina incompta and Globigerina bulloides as a surface water carbonate system proxy,
796 Earth Planet. Sci. Lett., 466, 139–151, 2017.

797 Rae, J.W.B.: Boron Isotopes in Foraminifera: Systematics, Biomineralisation, and CO_2
798 Reconstruction. In: Marschall, H., Foster, G. (eds), Boron Isotopes. Advances in Isotope
799 Geochemistry. Springer, Cham, 2018.

800 Rae, J. W. B., Foster, G. L., Schmidt, D. N. and Elliott, T.: Boron isotopes and B/Ca in benthic foraminifera:
801 Proxies for the deep ocean carbonate system, Earth Planet. Sci. Lett., 302, 403–413, 2011.

802 Raitzsch, M., Bijma, J., Benthien, A., Richter, K.-U., Steinhoefel, G. and Kučera, M.: Boron isotope-based
803 seasonal paleo-pH reconstruction for the Southeast Atlantic – A multispecies approach using habitat
804 preference of planktonic foraminifera, Earth Planet. Sci. Lett., 487, 138–150, 2018.

805 Ravelo, A. C. and Fairbanks, R. G.: Oxygen isotopic composition of multiple species of planktonic foraminifera:
806 recorder of the modern photic zone temperature gradient, Palaeogeogr. Palaeoclimatol. Palaeoecol., 7,
807 815–831, 1992.

808 Regenberg, M., Nürnberg, D., Steph, S., Groeneveld, J., Garbe-Schönberg, D., Tiedemann, R. and Dullo, W.-C.:
809 Assessing the effect of dissolution on planktonic foraminiferal Mg/Ca ratios: Evidence from Caribbean
810 core tops, Geochemistry, Geophys. Geosystems, 7, 2006.

811 Regenberg, M., Steph, S., Nürnberg, D., Tiedemann, R. and Garbe-Schönberg, D.: Calibrating Mg/Ca ratios of
812 multiple planktonic foraminiferal species with δ18O-calcification temperatures: Paleothermometry for the
813 upper water column, Earth Planet. Sci. Lett., 278, 324–336, 2009.

814 Rickaby, R. E. M. and Halloran, P.: Cool La Nina During the Warmth of the Pliocene?, Science, 307, 1948–
815 1952, 2005.

816 Ries, J. B., Cohen, A. L. and McCorkle, D. C.: Marine calcifiers exhibit mixed responses to CO2-induced ocean
817 acidification, Geology, 37, 1131–1134, 2009.

818 Rink, S., Kühl, M., Bijma, J. and Spero, H. J.: Microsensor studies of photosynthesis and respiration in the
819 symbiotic foraminifer Orbulina universa, Mar. Biol., 131, 583–595, 1998.

820 Rollion-Bard, C. and Erez, J.: Intra-shell boron isotope ratios in the symbiont-bearing benthic foraminiferan
821 Amphistegina lobifera: Implications for δ11B vital effects and paleo-pH reconstructions, Geochim.
822 Cosmochim. Acta, 74, 1530–1536, 2010.

823 Rostek, F., Ruhland, G., Bassinot, F. C., Muller, P. J., Labeyrie, L. D., Lancelot, Y. and Bard, E.: Reconstructing
824 Sea-Surface Temperature and Salinity Using δ18O and Alkenone Records, Nature, 364, 319–321, 1993.

825 Russell, A. D., Hönisch, B., Spero, H. J. and Lea, D. W.: Effects of seawater carbonate ion concentration and
826 temperature on shell U, Mg, and Sr in cultured planktonic foraminifera, Geochim. Cosmochim. Acta, 68,
827 4347–4361, 2004.

828 Sanyal, A., Bijma, J., Spero, H. J. and Lea, D. W.: Empirical relationship between pH and the boron isotopic
829 composition of Globigerinoides sacculifer: Implications for the boron isotopes paleo-pH proxy,
830 Paleoceanography, 16, 515–519, 2001.

https://doi.org/10.5194/bg-2019-266
Preprint. Discussion started: 8 August 2019

831 Sanyal, A., Hemming, N. G., Broecker, W. S., Lea, D. W., Spero, H. J., & Hanson, G. N. Oceanic pH control on
832 the boron isotopic composition of foraminifera: evidence from culture experiments, Paleoceanography,
833 11(5), 513-517, 1996.

834 Schmidt, G. A. and Mulitza, S.: Global calibration of ecological models for planktic foraminifera from coretop
835 carbonate oxygen-18, Mar. Micropaleontol., 44, 125–140, 2002.

836 Seki, O., Foster, G. L., Schmidt, D. N., Mackensen, A., Kawamura, K. and Pancost, R. D.: Alkenone and boron-
837 based Pliocene pCO2records, Earth Planet. Sci. Lett., 292, 201–211, 2010.

838 Shirayama, Y.: Effect of increased atmospheric CO2 on shallow water marine benthos, J. Geophys. Res., 110,
839 C09S08, 2005.

840 Sime, N. G., De La Rocha, C. L. and Galy, A.: Negligible temperature dependence of calcium isotope
841 fractionation in 12 species of planktonic foraminifera, Earth Planet. Sci. Lett., 232, 51–66, 2005.

842 Sutton, J. N., Liu, Y. W., Ries, J. B., Guillermic, M., Ponzevera, E. and Eagle, R. A.: δ11B as monitor of
843 calcification site pH in divergent marine calcifying organisms, Biogeosciences, 15, 1447–1467, 2018.

844 Thomson, J., Brown, L., Nixon, S., Cook, G. T. and MacKenzie, A. B.: Bioturbation and Holocene sediment
845 accumulation fluxes in the north-east Atlantic Ocean (Benthic Boundary Layer experiment sites), Mar.
846 Geol., 169, 21–39, 2000.

847 Tripati, A.: Deep-Sea Temperature and Circulation Changes at the Paleocene-Eocene Thermal Maximum.
848 Science, 308, 1894–1898, 2005.

849 Tripati, A. K., Roberts, C. D. and Eagle, R. A.: Coupling of CO2 and Ice Sheet Stability Over Major Climate
850 Transitions of the Last 20 Million Years, Science, 326, 1394–1397, 2009.

851 Tripati, A. K., Roberts, C. D., Eagle, R. A. and Li, G.: A 20 million year record of planktic foraminiferal B/Ca
852 ratios: Systematics and uncertainties in pCO2reconstructions, Geochim. Cosmochim. Acta, 75, 2582–
853 2610, 2011.

854 Uchikawa, J., Penman, D. E., Zachos, J. C. and Zeebe, R. E.: Experimental evidence for kinetic effects on B/Ca
855 in synthetic calcite: Implications for potential B(OH)4− and B(OH)3 incorporation, Geochim. Cosmochim.
856 Acta, 150, 171–191, 2015.

857 Urey, H.C., Lowenstam, H.A., Epstein, S. & McKinney, C.R.: Measurement of paleo-temperature and
858 temperatures of the upper cretaceous of England, Denmark, and the southeastern United-States. Geol. Soc.
859 Am. Bull., 62, 399-416, 1951.

860 Wang, B.-S., You, C.-F., Huang, K.-F., Wu, S.-F., Aggarwal, S. K., Chung, C.-H. and Lin, P.-Y.: Direct
861 separation of boron from Na- and Ca-rich matrices by sublimation for stable isotope measurement by MC-
862 ICP-MS, Talanta, 82, 1378–1384, 2010.

863 Wang, G., Cao, W., Yang, D. and Xu, D.: Variation in downwelling diffuse attenuation coefficient in the
864 northern South China Sea, Chinese J. Oceanol. Limnol., 26, 323–333, 2008.

865 Weare, B. C., Strub, P. T. and Samuel, M. D. Annual Mean Surface Heat Fluxes in the Tropical Pacific Ocean, J.
866 Phys. Oceanogr., 11, 705–717, 1981.

867 Wei, G., McCulloch, M. T., Mortimer, G., Deng, W. and Xie, L.: Evidence for ocean acidification in the Great
868 Barrier Reef of Australia, Geochim. Cosmochim. Acta, 73, 2332–2346, 2009.

869 Wilson, D. J., Piotrowski, A. M., Galy, A. and McCave, I. N.: A boundary exchange influence on deglacial
870 neodymium isotope records from the deep western Indian Ocean, Earth Planet. Sci. Lett., 341–344, 35–47,
871 2012.

https://doi.org/10.5194/bg-2019-266
Preprint. Discussion started: 8 August 2019

872 Wolf-Gladrow, D. A., Riebesell, U., Burkhardt, S. and Buma, J.: Direct effects of CO 2 concentration on growth
873 and isotopic composition of marine plankton, Tellus B Chem. Phys. Meteorol., 51, 461–476, 1999.

874 Yu, J., Menviel, L., Jin, Z. D., Thornalley, D. J. R., Barker, S., Marino, G., Rohling, E. J., Cai, Y., Zhang, F.,
875 Wang, X., Dai, Y., Chen, P. and Broecker, W. S.: Sequestration of carbon in the deep Atlantic during the
876 last glaciation, Nat. Geosci., 9, 319–324, 2016.

877 Yu, J., Foster, G. L., Elderfield, H., Broecker, W. S. and Clark, E.: An evaluation of benthic foraminiferal B/Ca
878 and δ11B for deep ocean carbonate ion and pH reconstructions, Earth Planet. Sci. Lett., 293, 114–120, 20.

879 Yu, J., Thornalley, D. J. R., Rae, J. W. B. and McCave, N. I.: Calibration and application of B/Ca, Cd/Ca, and δ
880 11 B in Neogloboquadrina pachyderma (sinistral) to constrain CO 2 uptake in the subpolar North Atlantic
881 during the last deglaciation, Paleoceanography, 28, 237–252, 2013.

882 Yu, J., Day, J., Greaves, M. and Elderfield, H., Determination of multiple element/calcium ratios in foraminiferal
883 calcite by quadrupole ICP-MS, Geochemistry, Geophys. Geosystems 6, 2005.

884 Zeebe, R. E. and Wolf-Gladrow, D., CO2 in Seawater: Equilibrium, Kinetics, Isotopes Elsevier Oceanography
885 Series 65, Amsterdam, 2001.

886 Zeebe, R. E., Wolf-Gladrow, D. A., Bijma, J. and Hönisch, B.,Vital effects in foraminifera do not compromise
887 the use of δ 11 B as a paleo- pH indicator: Evidence from modeling, Paleoceanography, 18, 2003.

https://doi.org/10.5194/bg-2019-266
Preprint. Discussion started: 8 August 2019

888 **Figure caption**

889

890 **Figure 1:** Reactions governing dissolved inorganic carbon equilibria**.**

891

892 **Figure 2:** (A) Speciation of H_3BO_3 and $H_4BO_4^-$ as function of seawater pH (total scale), (B) $\delta^{11}B$ of dissolved
893 inorganic boron species as a function of seawater pH, (C) sensitivity of $\delta^{11}B$ of $H_4BO_4^-$ for a pH ranging from
894 7.6 to 8.4. T=25°C, S=35, $\delta^{11}B$=39.61 ‰ (Foster et al., 2010), dissociation constant α = 1.0272 (Klochko et al.,
895 2006).

896

897 **Figure 3:** Map showing locations of the core-tops used in this study (white diamonds). Red open circles
898 represent the sites used for in-situ carbonate parameters from GLODAP database (Key et al., 2004).

899

900 **Figure 4:** Pre-industrial data versus depth of the sites used in this study. The figure shows seasonal temperatures
901 (extracted from World Ocean Database 2013), density anomaly (kg/m^3), pre-industrial pH and pre-industrial
902 $\delta^{11}B$ of $H_4BO_4^-$ (calculated from the GLODAP database and corrected for anthropogenic inputs).

903

904 **Figure 5:** Boron isotopic measurements of mixed-layer foraminifera plotted against the $\delta^{11}B_{borate}$. $\delta^{11}B_{borate}$ were
905 characterized by determination of the calcification depth of the foraminifera, A) *G. ruber*, B) *T. sacculifer*, C) *O.*
906 *universa*. Mono-specific calibrations are summarized in Table 3.

907

908 **Figure 6:** Boron isotopic measurements of deep-dwelling foraminifera ($\delta^{11}B_{carbonate}$) plot against $\delta^{11}B_{borate}$.
909 $\delta^{11}B_{borate}$ were characterized by determining the calcification depth of foraminifera, A) *P. obliquiloculata*, B) *G.*
910 *menardii*, C) *N. dutertrei*, D) *G. tumida* and E) Compilation of deep dweller species. Mono-specific calibrations
911 are summarized in Table 3.

912

913 **Figure 7:** Light penetration profile in the Western Pacific, with E_0 in the WEP of 220 J.s-1.m-2 (Weare et al.,
914 1981) and a light attenuation coefficient of 0.028 (Wang et al., 2008). Theoretical depth were calculated for a
915 decrease in micro-environment pH of ΔpH_1= -0.04, ΔpH_2= -0.06. Light penetration corresponding to Ec is
916 ~12%, ΔpH_1 ~5% , ΔpH_2 ~1% respective depth are 75m, 110m and 150m. Green band is the calcification depth
917 of *T. sacculifer* (w/o sacc) utilized in this study.

918

919 **Figure 8:** Water depth pH profiles reconstructed at every site applying the mono-specific calibrations derived
920 from our results (Table 3). Figure is showing measured $\delta^{11}B_{calcite}$, $\delta^{11}B_{borate}$ calculated according to different
921 calibrations (see Table 3 and text), calculated pH based on $\delta^{11}B$ ($pH_{\delta 11B}$) and pCO_2 calculated from $pH_{\delta 11B}$ and
922 alkalinity.

923

924

925

https://doi.org/10.5194/bg-2019-266
Preprint. Discussion started: 8 August 2019

Table caption

Table 1: Box-core information

Table 2: Analytical results of $\delta^{13}C$, $\delta^{18}O$, $\delta^{11}B$ and elemental ratios Li/Ca, B/Ca and Mg/Ca

Table 3: Mono specific $\delta^{11}B_{carbonate}$ to $\delta^{11}B_{borate}$ calibrations from literature and from our data

https://doi.org/10.5194/bg-2019-266
Preprint. Discussion started: 8 August 2019

Biogeosciences
Discussions
Open Access
EGU

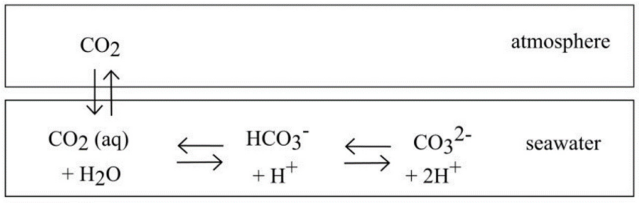

Figure 1

https://doi.org/10.5194/bg-2019-266
Preprint. Discussion started: 8 August 2019

Biogeosciences
Discussions
Open Access
EGU

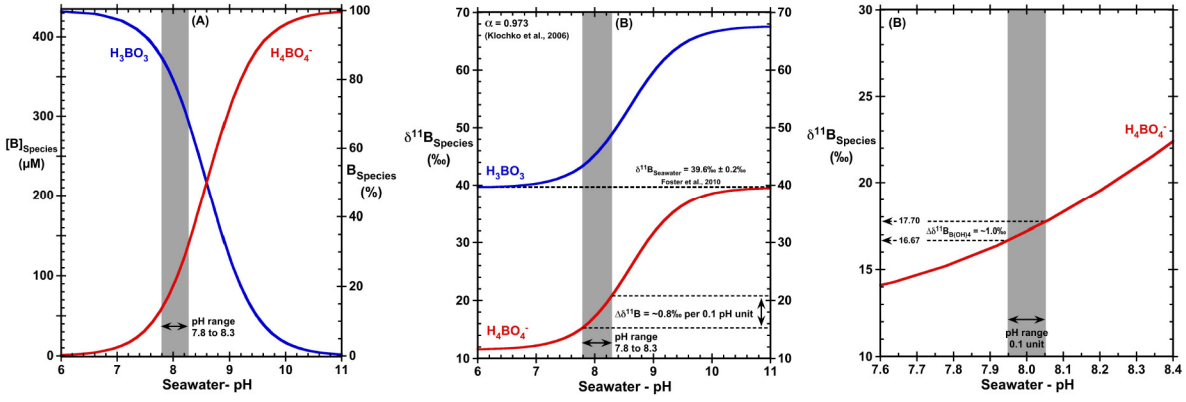

Figure 2

https://doi.org/10.5194/bg-2019-266
Preprint. Discussion started: 8 August 2019

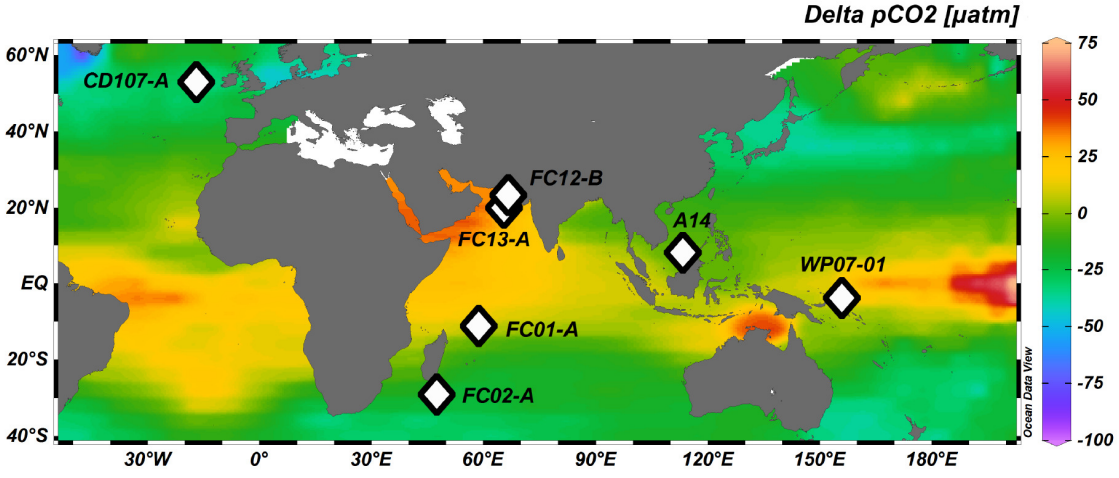

Figure 3

https://doi.org/10.5194/bg-2019-266
Preprint. Discussion started: 8 August 2019

Biogeosciences
Discussions
Open Access
EGU

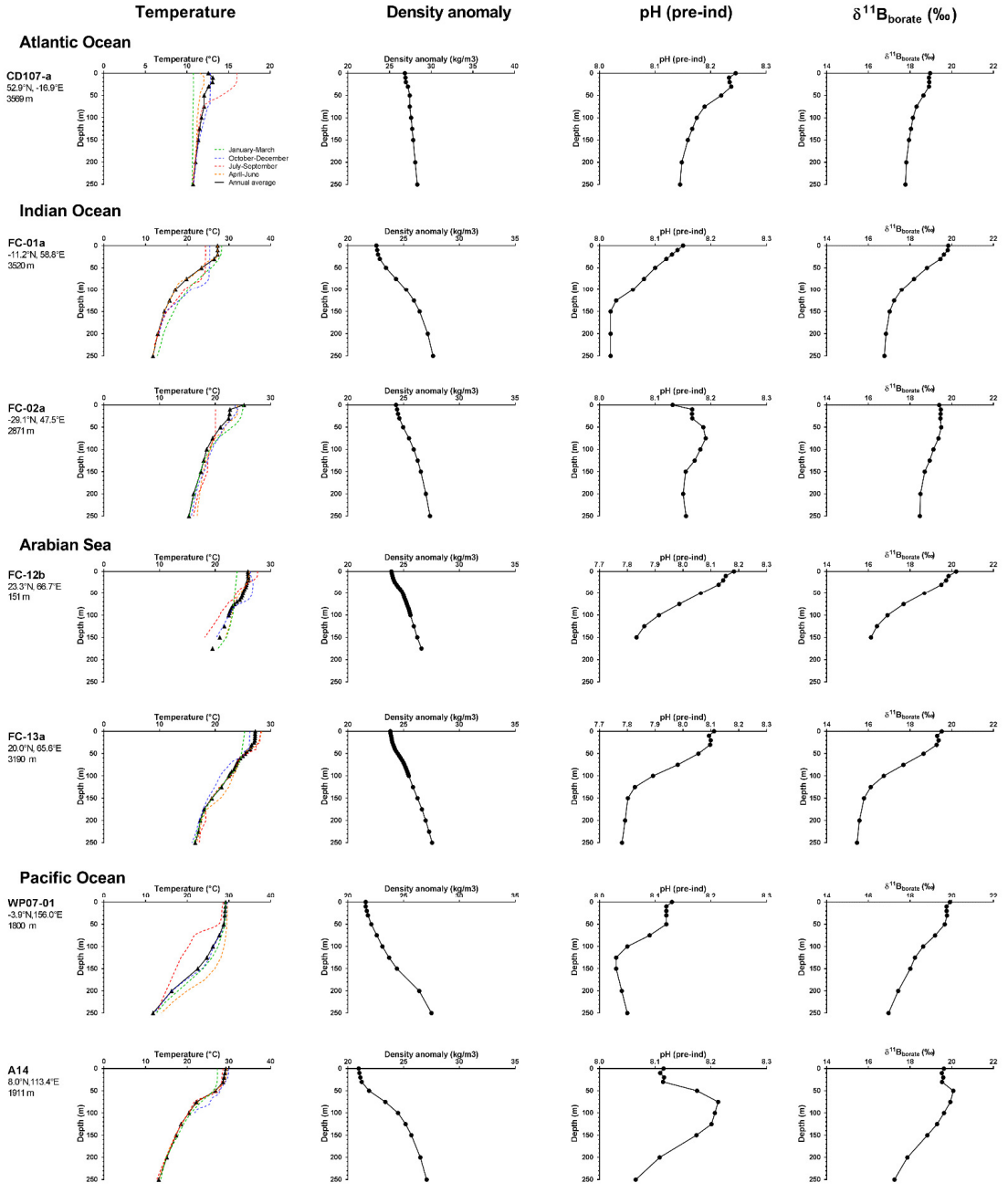

Figure 4

https://doi.org/10.5194/bg-2019-266
Preprint. Discussion started: 8 August 2019

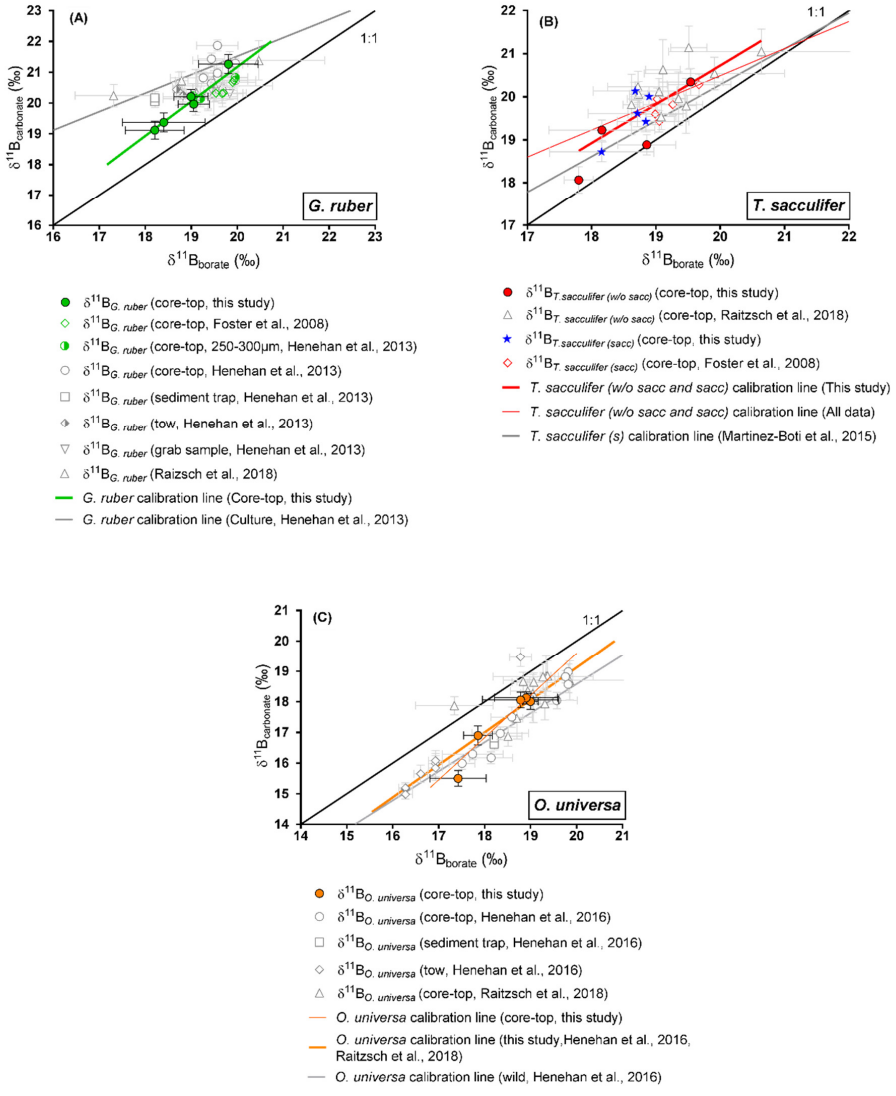

Figure 5

https://doi.org/10.5194/bg-2019-266
Preprint. Discussion started: 8 August 2019

Biogeosciences
Discussions
Open Access
EGU

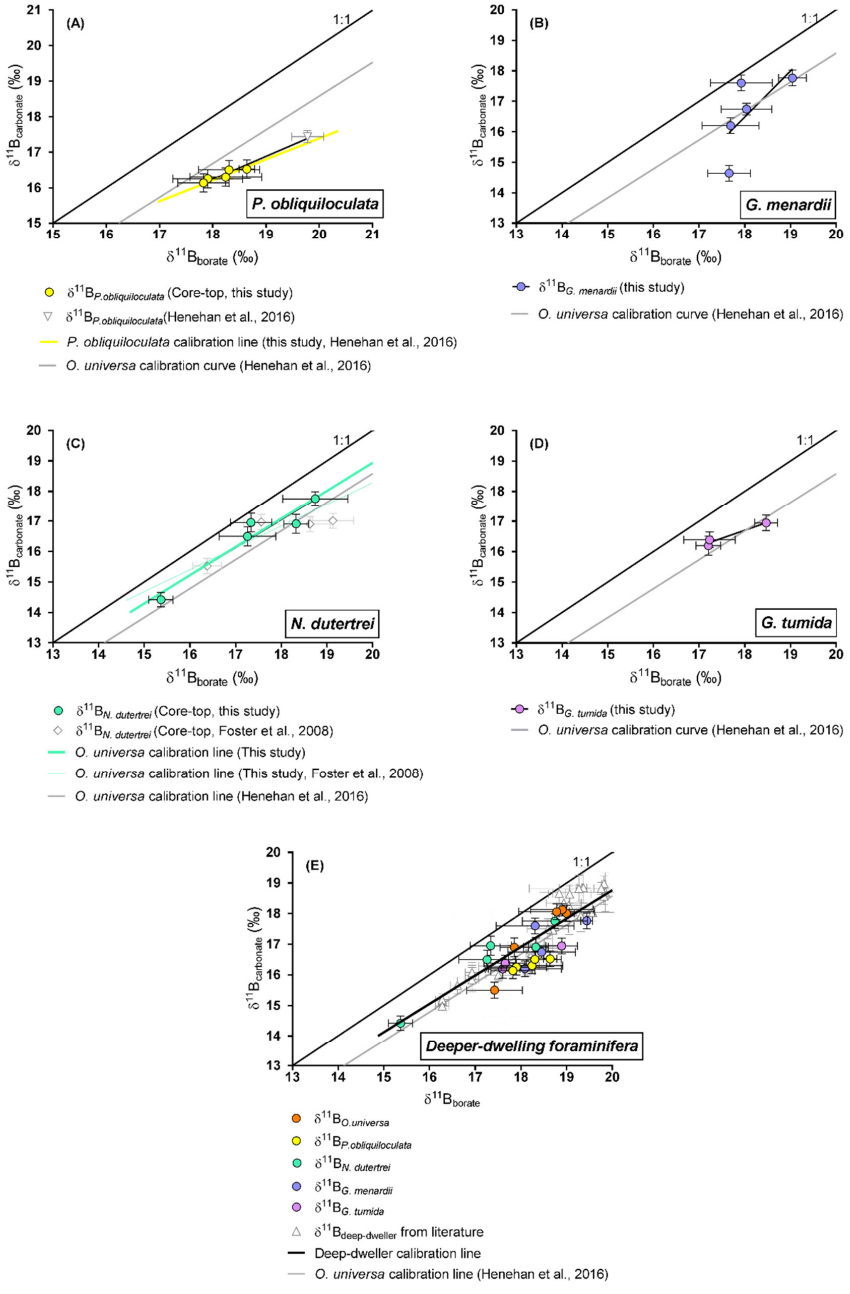

Figure 6

https://doi.org/10.5194/bg-2019-266
Preprint. Discussion started: 8 August 2019

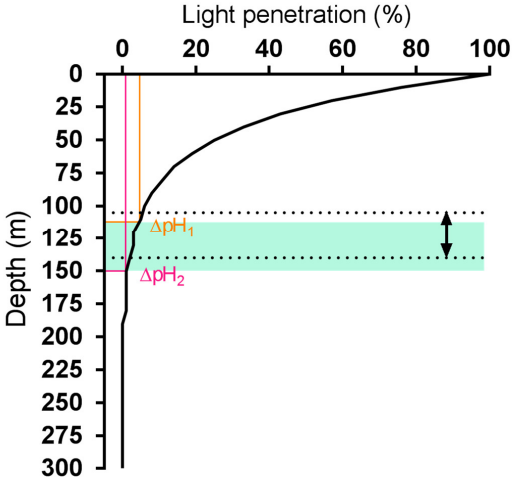

Figure 7

https://doi.org/10.5194/bg-2019-266
Preprint. Discussion started: 8 August 2019

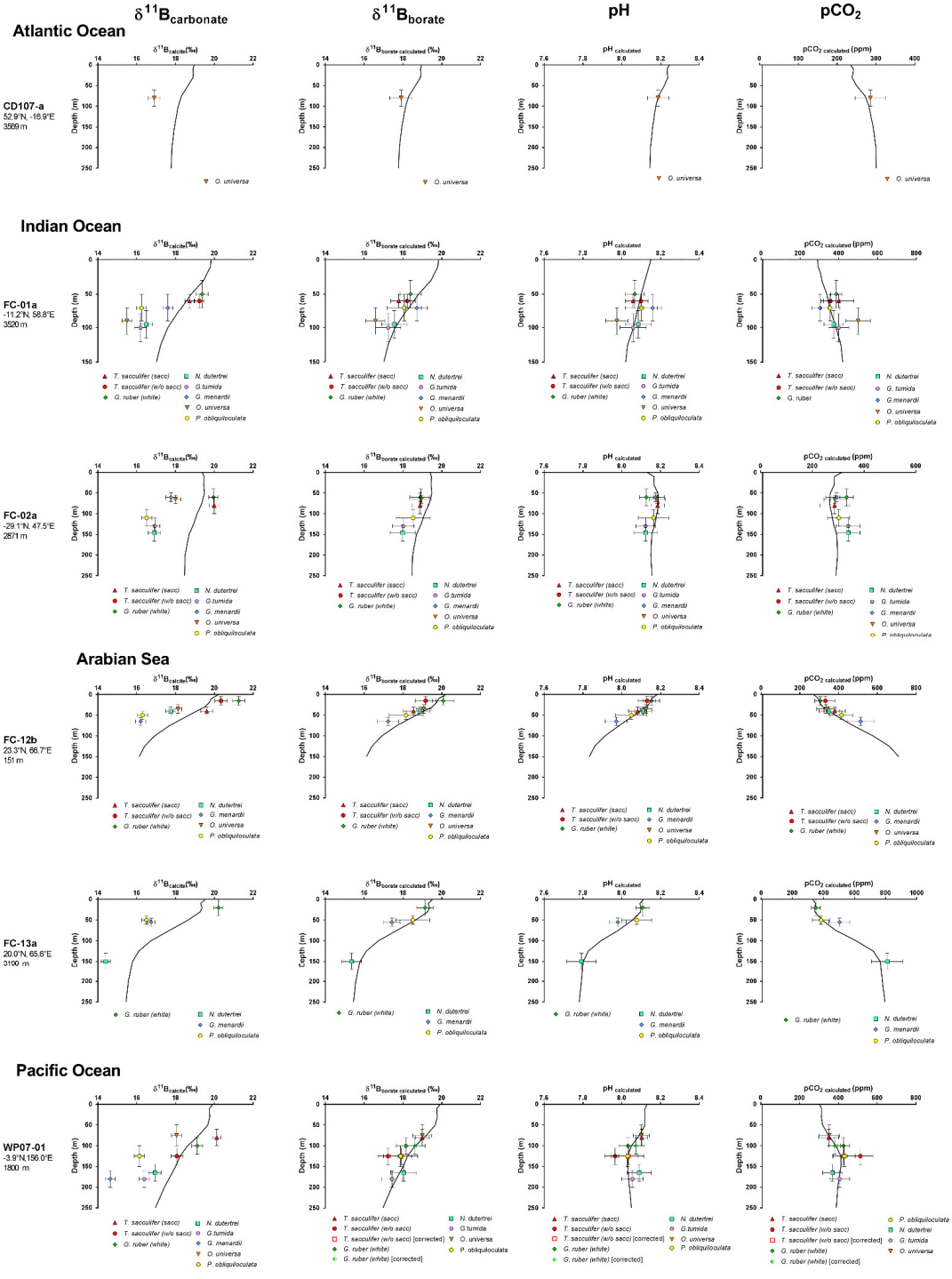

Figure 8

https://doi.org/10.5194/bg-2019-266
Preprint. Discussion started: 8 August 2019

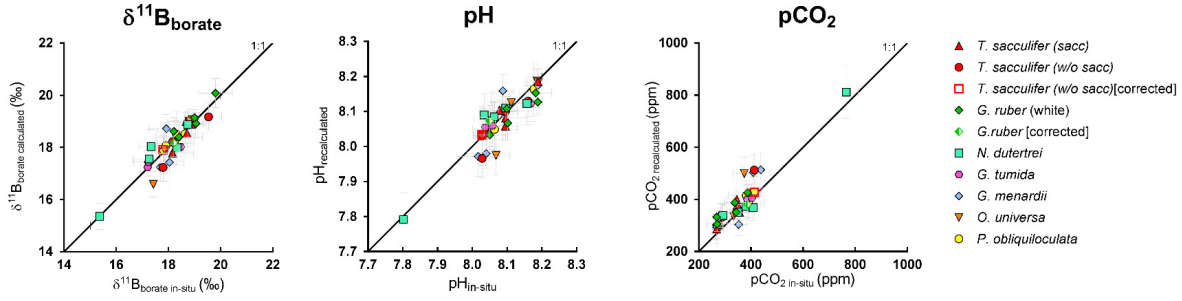

Figure 9

https://doi.org/10.5194/bg-2019-266
Preprint. Discussion started: 8 August 2019

Biogeosciences Discussions
Open Access
EGU

Table 1

Label	Box-Core	Site	Latitude (N)	Longitude (E)	Depth (mbsl)	Oceanic Regime	$\Delta^{14}C$ age (year)
Atlantic Ocean							
CD107-a	CD107	A	52.92	-16.92	3569	non-upwelling	<3000[a]
Indian Ocean							
FC-01a	WIND-33B	I	-11.21	58.77	3520	non-upwelling	
FC-02a	WIND-10B	K	-29.12	47.55	2871	non-upwelling	7252 ± 27[b]
Arabian Sea							
FC-12b	CD145	A150	23.30	66.70	151	seasonal upwelling	
FC-13a	CD145	A3200	20.00	65.58	3190	seasonal upwelling	
Pacific Ocean							
WP07-01			-3.93	156.00	1800	non-upwelling	7.3-8.6[c]
A14			8.02	113.39	1911	non-upwelling	

[a] Thomson et al., 2000
[b] Wilson et al., 2012
[c] Age for core-top of site 806B from Lea et al., 2000

https://doi.org/10.5194/bg-2019-266
Preprint. Discussion started: 8 August 2019

Biogeosciences Discussions Open Access EGU

Table 2

Core	Species	Fraction size (µm)	Cleaning	$\delta^{13}C$*	$\delta^{18}O$*	$\delta^{11}Bc_1$	$\delta^{11}Bc_2$	$\delta^{11}B_{average}$**	Li/Ca***	B/Ca***	Mg/Ca***
				(‰)	(‰)	(‰)	(‰)	(‰)	(µmol/mol)	(µmol/mol)	(mmol/mol)
Atlantic Ocean											
CD107a	*O. universa*	>500	Ox-Red	1.99 ± 0.03	1.25 ± 0.11	16.85 ± 0.31 (2SD, nAE121=11)	16.95 ± 0.31 (2SD, nAE121=11)	16.90 ± 0.22	13.9 ± 0.4	68 ± 7	3.60 ± 0.01
Indian Ocean											
FC-01a	*G. ruber (white ss)*	250-300	Ox-Red	1.37 ± 0.03	-1.32 ± 0.11	19.33 ± 0.31 (2SD, nAE121=11)	19.41 ± 0.31 (2SD, nAE121=11)	19.37 ± 0.22	15.4 ± 0.4	109 ± 7	3.98 ± 0.01
FC-01a	*T. sacculifer (sacc)*	300-400	Ox-Red	1.88 ± 0.03	-2.20 ± 0.11	18.71 ± 0.24 (2SD, nAE121=10)	18.73 ± 0.24 (2SD, nAE121=10)	18.72 ± 0.17	12.1 ± 0.4	87 ± 7	3.45 ± 0.01
FC-01a	*T. sacculifer (w/o sacc)*	300-400	Ox-Red	2.02 ± 0.03	-1.05 ± 0.11	19.13 ± 0.24 (2SD, nAE121=10)	19.32 ± 0.24 (2SD, nAE121=10)	19.23 ± 0.17	12.1 ± 0.4	82 ± 7	3.42 ± 0.01
FC-01a	*O. universa*	>500	Ox-Red			15.50 ± 0.26 (2SD, nAE121=14)		15.50 ± 0.26			
FC-01a	*P. obliquiloculata*	300-400	Ox-Red	1 .00± 0.03	-0.55 ± 0.11	16.40 ± 0.26 (2SD, nAE121=14)	16.10 ± 0.26 (2SD, nAE121=14)	16.25 ± 0.18	15.4 ± 0.4	78 ± 7	2.06 ± 0.01
FC-01a	*G. menardii*	300-400	Ox-Red	1.64 ± 0.03	0.43 ± 0.11	17.52 ± 0.26 (2SD, nAE121=14)	17.69 ± 0.26 (2SD, nAE121=14)	17.60 ± 0.18	12.7 ± 0.4	63 ± 7	2.26 ± 0.01
FC-01a	*N. dutertrei*	300-400	Ox-Red	1.28 ± 0.03	-0.43 ± 0.11	16.40 ± 0.31 (2SD, nAE121=11)	16.59 ± 0.31 (2SD, nAE121=11)	16.50 ± 0.22	18.6 ± 0.4	73 ± 7	1.81 ± 0.01
FC-01a	*G. tumida*	300-400	Ox-Red	1.29 ± 0.03	-0.53 ± 0.11	16.21 ± 0.31 (2SD, nAE121=11)	16.18 ± 0.31 (2SD, nAE121=11)	16.20 ± 0.22	10.0 ± 0.4	61 ± 7	1.79 ± 0.01
FC-02a	*G. ruber (white ss)*	250-300	Ox-Red	0.30 ± 0.03	-1.40 ± 0.11	20.02 ± 0.24 (2SD, nAE121=10)	19.90 ± 0.24 (2SD, nAE121=10)	19.96 ± 0.17	18.2 ± 0.4	125 ± 7	3.47 ± 0.01
FC-02a	*T. sacculifer (sacc)*	300-400	Ox-Red	1.43 ± 0.03	-1.60 ± 0.11	20.07 ± 0.24 (2SD, nAE121=10)	19.93 ± 0.24 (2SD, nAE121=10)	20.00 ± 0.17	14.2 ± 0.4	106 ± 7	3.30 ± 0.01
FC-02a	*T. sacculifer (w/o sacc)*	300-400	Ox-Red	1.52 ± 0.03	-1.40 ± 0.11	23.23 ± 0.24 (2SD, nAE121=10)	23.22 ± 0.24 (2SD, nAE121=10)	23.22 ± 0.17	13.7 ± 0.4	106 ± 7	3.34 ± 0.01
FC-02a	*O. universa*	>500	Ox-Red	1.79 ± 0.03	0.02 ± 0.11	18.05 ± 0.26 (2SD, nAE121=14)	17.97 ± 0.26 (2SD, nAE121=14)	18.01 ± 0.18	14.8 ± 0.4	67 ± 7	4.40 ± 0.01
FC-02a	*P. obliquiloculata*	300-400	Ox-Red	0.34 ± 0.03	0.56 ± 0.11	16.35 ± 0.26 (2SD, nAE121=14)	16.69 ± 0.26 (2SD, nAE121=14)	16.52 ± 0.18	16.6 ± 0.4	83 ± 7	2.33 ± 0.01
FC-02a	*G. menardii*	300-400	Ox-Red	1.73 ± 0.03	-0.51 ± 0.11	17.77 ± 0.26 (2SD, nAE121=14)		17.77 ± 0.26	15.8 ± 0.4	125 ± 7	2.21 ± 0.01
FC-02a	*N. dutertrei*	300-400	Ox-Red	1.03 ± 0.03	-0.55 ± 0.11	16.78 ± 0.31 (2SD, nAE121=11)	17.03 ± 0.31 (2SD, nAE121=11)	16.91 ± 0.22	18.6 ± 0.4	82 ± 7	2.13 ± 0.01
FC-02a	*G. tumida*	300-400	Ox-Red	1.64 ± 0.03	-0.28 ± 0.11	16.93 ± 0.26 (2SD, nAE121=14)	16.95 ± 0.26 (2SD, nAE121=14)	16.94 ± 0.18	15.6 ± 0.4	87 ± 7	1.90 ± 0.01
Arabian Sea											
FC-12b	*G. ruber (white ss)*	250-300	Ox-Red	0.58 ± 0.03	-2.82 ± 0.11	21.30 ± 0.31 (2SD, nAE121=11)	21.23 ± 0.31 (2SD, nAE121=11)	21.26 ± 0.22	19.5 ± 0.4	164 ± 7	5.76 ± 0.01
FC-12b	*G. sacculifer (s)*	300-400	Ox-Red	1.76 ± 0.03	-2.15 ± 0.11	19.65 ± 0.31 (2SD, nAE121=11)	19.57 ± 0.31 (2SD, nAE121=11)	19.61 ± 0.22	14.6 ± 0.4	101 ± 7	4.28 ± 0.01
FC-12b	*T. sacculifer (w/o sacc)*	300-400	Ox-Red	1.97 ± 0.03	-2.19 ± 0.11	20.32 ± 0.31 (2SD, nAE121=11)	20.37 ± 0.31 (2SD, nAE121=11)	20.34 ± 0.22	16.7 ± 0.4	116 ± 7	4.90 ± 0.01
FC-12b	*O. universa*	>500	Ox-Red	1.89 ± 0.03	-1.59 ± 0.11	18.13 ± 0.20 (2SD, nAE121=6)		18.13 ± 0.20	13.6 ± 0.4	103 ± 7	6.91 ± 0.01
FC-12b	*P. obliquiloculata*	300-400	Ox-Red	0.5 ± 0.03	-1.58 ± 0.11	16.45 ± 0.26 (2SD, nAE121=14)	16.15 ± 0.26 (2SD, nAE121=14)	16.30 ± 0.18	16.7 ± 0.4	95 ± 7	3.61 ± 0.01
FC-12b	*G. menardii*	300-400	Ox-Red	1.05 ± 0.03	-0.97 ± 0.11	16.2 ± 0.26 (2SD, nAE121=14)		16.20 ± 0.26	14.8 ± 0.4	75 ± 7	3.44 ± 0.01
FC-12b	*N. dutertrei*	300-400	Ox-Red	1.35 ± 0.03	-1.57 ± 0.11	17.77 ± 0.24 (2SD, nAE121=10)	17.73 ± 0.24 (2SD, nAE121=10)	17.75 ± 0.17	17.1 ± 0.4	75 ± 7	3.25 ± 0.01
FC-13a	*G. ruber (white ss)*	250-300	Ox-Red	0.08 ± 0.03	-3.71 ± 0.11	20.27 ± 0.24 (2SD, nAE121=10)	20.15 ± 0.24 (2SD, nAE121=10)	20.21 ± 0.17	16.4 ± 0.4	147 ± 7	4.52 ± 0.01
FC-13a	*T. sacculifer (w/o sacc)*	300-400	Ox-Red	1.59 ± 0.03	-2.46 ± 0.11	17.85 ± 0.29 (2SD, nAE121=12)		17.85 ± 0.29	15.7 ± 0.4	121 ± 7	5.49 ± 0.01
FC-13a	*P. obliquiloculata*	300-400	Ox-Red	0.00 ± 0.03	-0.97 ± 0.11	16.51 ± 0.26 (2SD, nAE121=14)	16.50 ± 0.26 (2SD, nAE121=14)	16.51 ± 0.18	18.7 ± 0.4	79 ± 7	4.43 ± 0.01
FC-13a	*G. menardii*	300-400	Ox-Red	0.75 ± 0.03	-1.07 ± 0.11	16.74 ± 0.20 (2SD, nAE121=6)		16.74 ± 0.20	9.2 ± 0.4	60 ± 7	1.99 ± 0.01
FC-13a	*N. dutertrei*	300-400	Ox-Red	0.71 ± 0.03	-1.41 ± 0.11	14.43 ± 0.24 (2SD, nAE121=10)	14.40 ± 0.24 (2SD, nAE121=10)	14.41 ± 0.17	15.7 ± 0.4	69 ± 7	1.98 ± 0.01
Pacific Ocean											
WP07-a	*G. ruber (white ss)*	250-400	Ox-Red			19.12 ± 0.29 (2SD, nAE121=12)		19.12 ± 0.29	14.5 ± 0.4	144 ± 7	4.32 ± 0.01
WP07-a	*T. sacculifer (sacc)*	250-400	Ox-Red			20.13 ± 0.21 (2SD, nAE121=11)		20.13 ± 0.21	12.7 ± 0.4	92 ± 7	4.44 ± 0.01
WP07-a	*T. sacculifer (w/o sacc)*	250-400	Ox-Red			18.10 ± 0.31 (2SD, nAE121=11)	18.04 ± 0.31 (2SD, nAE121=11)	18.07 ± 0.22	12.3 ± 0.4	192 ± 7	4.51 ± 0.01
WP07-a	*O.universa*	500-630	Ox-Red			18.13 ± 0.26 (2SD, nAE121=14)	17.99 ± 0.26 (2SD, nAE121=14)	18.06 ± 0.18	11.9 ± 0.4	71 ± 7	7.52 ± 0.01
WP07-a	*P. obliquiloculata*	250-400	Ox-Red			16.08 ± 0.26 (2SD, nAE121=14)	16.19 ± 0.26 (2SD, nAE121=14)	16.14 ± 0.18	13.4 ± 0.4	72 ± 7	3.02 ± 0.01
WP07-a	*G. menardii*	250-400	Ox-Red			14.74 ± 0.26 (2SD, nAE121=14)	14.53 ± 0.26 (2SD, nAE121=14)	14.64 ± 0.18	13.5 ± 0.4	85 ± 7	2.68 ± 0.01
WP07-a	*N. dutertrei*	250-400	Ox-Red			16.91 ± 0.31 (2SD, nAE121=11)	16.99 ± 0.31 (2SD, nAE121=11)	16.95 ± 0.22	21.7 ± 0.4	86 ± 7	3.66 ± 0.01
WP07-a	*G. tumida*	250-400	Ox-Red			16.45 ± 0.26 (2SD, nAE121=14)	16.32 ± 0.26 (2SD, nAE121=14)	16.39 ± 0.18	10.6 ± 0.4	58 ± 7	2.55 ± 0.01
A14	*G. ruber (white ss)*	250-400	Ox-Red			18.91 ± 0.24 (2SD, nAE121=10)	19.17 ± 0.24 (2SD, nAE121=10)	19.04 ± 0.17			
A14	*T. sacculifer (sacc)*	250-400	Ox-Red			19.53 ± 0.24 (2SD, nAE121=10)	19.32 ± 0.24 (2SD, nAE121=10)	19.42 ± 0.17	12.0 ± 0.4	102 ± 7	3.91 ± 0.01
A14	*T. sacculifer (w/o sacc)*	250-400	Ox-Red			18.93 ± 0.24 (2SD, nAE121=10)	18.84 ± 0.24 (2SD, nAE121=10)	18.88 ± 0.17	12.3 ± 0.4	93 ± 7	3.76 ± 0.01
A14	*O. universa*	500-560	Ox-Red			17.33 ± 0.26 (2SD, nAE121=14)	17.08 ± 0.26 (2SD, nAE121=14)	17.20 ± 0.18	11.3 ± 0.4	66 ± 7	6.59 ± 0.01
A14	*N. dutertrei*	250-400	Ox-Red			14.39 ± 0.31 (2SD, nAE121=11)		14.39 ± 0.31	16.9 ± 0.4	75 ± 7	1.99 ± 0.01

* uncertainties given in 1SD (see text)

** When two measurements were carried out uncertaity was calculated with $\Delta a = \sqrt{(1/\sum_i (1/\Delta_{ai})^2)}$; with only one measurement the error was determined on reproducibility of the AE121 standard

***Uncertainty given in 2SD , calculated on the reproducibility of CamWuellestorfi (see text and table S3, ref in Misra et al., 2014)

https://doi.org/10.5194/bg-2019-266
Preprint. Discussion started: 8 August 2019

Biogeosciences Discussions
Open Access
EGU

Table 3

Species	Size fraction (µm)	Material	Instrument (original)	$\delta^{11}B_{borate}$= f($\delta^{11}B_{calcite}$)	R^2	p	n	Calibration number	Reference
G. ruber	~ 250	Culture/core tops/plankton tows	MC-ICP-MS	$\delta^{11}B_{borate}$=[$\delta^{11}B_{calcite}$ - 9.52 (±2.02)]/0.6 (±0.11)					Henehan et al., 2013
G. ruber	315-355	Core-tops	MC-ICP-MS	$\delta^{11}B_{borate}$=[$\delta^{11}B_{calcite}$ - 11.78 (±3.20)]/0.45 (±0.16)					Raitzsch et al., 2018
T. sacculifer	n.d.	Culture/artificial seawater enriched in B	N-TIMS	$\delta^{11}B_{borate}$=[$\delta^{11}B_{calcite}$ - 3.94 (±4.02)]/0.82 (±0.22)					Sanyal et al., 2001 refitted Martinez-Boti et al., 2015
T. sacculifer	315-355	Core-tops	MC-ICP-MS	$\delta^{11}B_{borate}$=[$\delta^{11}B_{calcite}$ - 8.86 (±5.27)]/0.59 (±0.21)					Raitzsch et al., 2018
O. universa	no effect	Core-tops/plankton tows/sediment traps	MC-ICP-MS	$\delta^{11}B_{borate}$=[$\delta^{11}B_{calcite}$ + 0.42 (±2.85)]/0.95 (±0.17)					Henehan et al., 2016
O. universa	>425	Core-tops	MC-ICP-MS	$\delta^{11}B_{borate}$=[$\delta^{11}B_{calcite}$ + 5.69 (±7.51)]/1.26 (±0.39)					Raitzsch et al., 2018
G. bulloides	300-355	Core-top/sediment trap	MC-ICP-MS	$\delta^{11}B_{borate}$=[$\delta^{11}B_{calcite}$ + 3.440 (±4.584)]/1.074 (±0.252)					Martínez-Botí et al., 2015
G. bulloides	315-355	Core-tops	MC-ICP-MS	$\delta^{11}B_{borate}$=[$\delta^{11}B_{calcite}$ + 3.81 (±13.17)]/1.13 (±0.72)					Raitzsch et al., 2018
N. pachyderma	150-200	Core-tops	MC-ICP-MS	$\delta^{11}B_{borate}$= $\delta^{11}B_{calcite}$ + 3.38					Yu et al., 2013
G. ruber	250-400	Core-tops	MC-ICP-MS	$\delta^{11}B_{borate}$=[$\delta^{11}B_{calcite}$ + 1.23 (±0.59)]/1.12(±1.67)	0.975	0.002	5	**1**	This study
T. sacculifer (sacc and	250-400	Core-tops	MC-ICP-MS	$\delta^{11}B_{borate}$=[$\delta^{11}B_{calcite}$ + 2.09 (± 14.31)/1.17 (± 2.11)	0.652	0.009	9	**2**	This study
T. sacculifer (sacc and	250-400	Core-tops	MC-ICP-MS	$\delta^{11}B_{borate}$=[$\delta^{11}B_{calcite}$ - 7.89 (±1.70)]/0.63(±0.56)	0.594	<0.0001	25	**3**	This study; Foster et al., 2008; Raitzsch et al., 2018
N. dutertrei	300-400	Core-tops	MC-ICP-MS	$\delta^{11}B_{borate}$=[$\delta^{11}B_{calcite}$ - 0.34 (±1.83)]/0.93 (±0.55)	0.918	0.010	5	**4**	This study
N. dutertrei	300-400	Core-tops	MC-ICP-MS	$\delta^{11}B_{borate}$=[$\delta^{11}B_{calcite}$ - 3.88 (±0.65)]/0.72 (±0.74)	0.795	0.001	9	**5**	This study; Foster et al., 2008
O. universa	400-600	Core-tops	MC-ICP-MS	$\delta^{11}B_{borate}$=[$\delta^{11}B_{calcite}$ + 8.01 (±23)]/1.38 (±2.67)	0.897	0.015	5	**6**	This study
O. universa	400-600	Core-tops	MC-ICP-MS	$\delta^{11}B_{borate}$=[$\delta^{11}B_{calcite}$ + 2.08 (±0.59)]/1.06 (±0.13)	0.932	0.008	5	**7**	This study; Henehan et al., 2016; Raitzsch et al., 2018
G. menardii	400-600	Core-tops	MC-ICP-MS	$\delta^{11}B_{borate}$=[$\delta^{11}B_{calcite}$ - 5.36 (±1.36)]/0.65 (±0.76)	0.460	0.208	5	**8**	This study
G. tumida	400-600	Core-tops	MC-ICP-MS	$\delta^{11}B_{borate}$=[$\delta^{11}B_{calcite}$ - 6.33 (±2.52)]/0.57 (±1.2)	0.948	0.146	3	**9**	This study
P. obliquiloculata	300-400	Core-tops	MC-ICP-MS	$\delta^{11}B_{borate}$=[$\delta^{11}B_{calcite}$ - 5.59 (±4.16)]/0.59(±0.65)	0.965	0.001	6	**10**	This study; Henehan et al., 2016
Deep-dweller	300-600	Core-tops	MC-ICP-MS	$\delta^{11}B_{borate}$=[$\delta^{11}B_{calcite}$ -1.99 (±0.13)]/0.82 (±0.27)	0.686	<0.0001	22	**11**	This study
Deep-dweller	300-600	Core-tops	MC-ICP-MS	$\delta^{11}B_{borate}$=[$\delta^{11}B_{calcite}$ - 0.18 (±0.6)]/0.95 (±0.13)	0.800	<0.0001	54	**12**	This study; Foster et al., 2008; Henehan et al., 2016; Raitzsch et al., 2018